

Concentrating Solar Power (CSP) field, Losses, Mathematics involved and Non-Imaging Optics

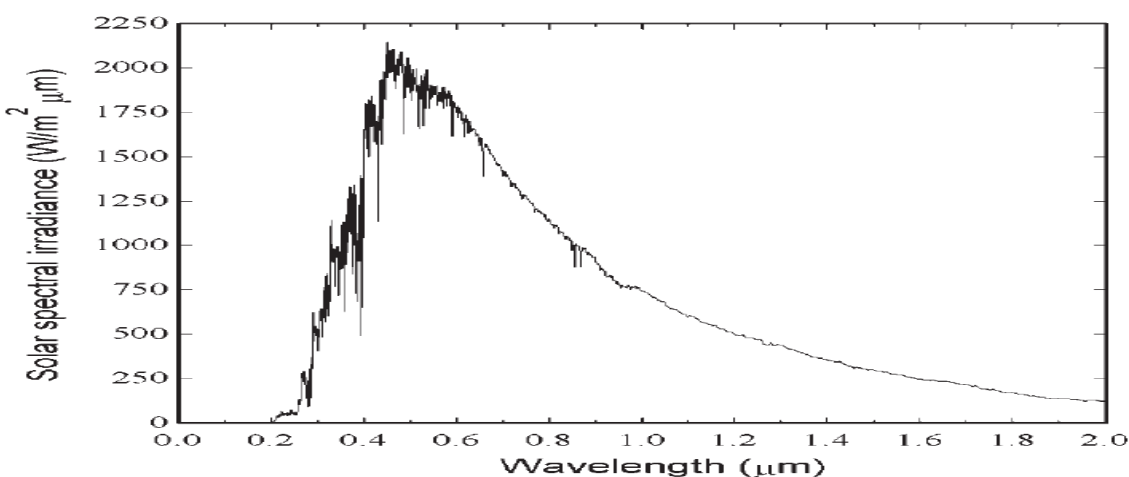


Fig 3.1: Solar spectrum [74]

The above figure 3.1 depicts the observed solar spectrum before the Earth's atmosphere. As in figure 3.1 (and in fig 2.5 before) the Sun has the predominant emission in the range of greenish-yellow color (500-565 nm). As a hot body at $\sim 5600 \text{ K}$, sun emits electromagnetic radiation with a definite spectral space i.e the blue curve above. According to Planck's law, peak frequency f of any spectrum is proportional to the absolute temperature T and its peak wavelength λ is inversely proportional to T (Wein's law).

While radiating back, the surface of the Earth radiates at $\sim 300 \text{ K}$ and its thermal radiation peaks in the far infrared.

3.1 Heliostats and CSP field design

3.1.1 Heliostats

A Heliostat is a highly reflective, may be curved, mirror usually placed on the ground or close to it. It acts as a reflector of the Solar rays and hence participate in forming solar images on the receiver/detector, elevated. Being a mirror, depending on the radius of curvature, it generates

a calculated focal point/spot on the receiver. Apart from high reflectivity, Heliostats are supposed to have following properties [96,97]:

- a. It is supposed to have high optical precision.
- b. To direct the solar rays to the receiver throughout the day, depending on the Azimuth and altitude angle of the Sun, the tracking accuracy of the Heliostats are supposed to be high.
- c. As the entire bed of the Heliostats rest on the ground and supposed to face the sun throughout the day it is necessary for individual Heliostats to have a resistant surface.

A heliostat, being a concave mirror, is an equivalent to a positive lens and hence forms a real image of any distant object. Although, mathematically, it generates an inverted image, Sun being considered as a circular object in 2d, Heliostat produce an image which replicates the Solar shape.

As an imaging device, Heliostat follows sign convention as below

- a. The sign of the indices reverse on reflection. As a consequence, index, as after reflection the rays travel in opposite direction, changes sign.
- b. Spacing between elements, in this case, Heliostats and receiver, changes sign as direction of ray trace change.

In a conventional manner, Solar rays toward the Heliostats are considered as positive and rays away from Heliostats i.e towards the receiver are considered as negative. Accordingly, the radius of curvature and hence the focal length of the heliostat's surface are considered is (-) ive.

In case of beam down optical concentration, because of two reflective elements, the sign change happens twice and the final position of focal spot depends on the nature of surface of the secondary surface.

Concentrating Solar Power is a manner of work where highly reflective opticelements namely mirrors, are placed on the ground with a specified layout. These primary mirrors are to be oriented with calculated tilt and curvature to take the radiation to a predetermined receiver position, highly absorptive and the heat absorbed is unitized to heat up normal temperature water or a salt mixer. The water would form steam or a Heat Transfer Fluid (HTF) will carry the heat from the salt for generation of steam. A steam turbine is made to rotate at requisite speed because of high temperature and high pressure associated with steam and using appropriate conversion equipment's electricity can be generated.

Heat Energy, as it may be stored, is utilized for current and later usage.

At times when solar energy is not available, for instance during night and during cloud cover, the stored heat energy may be used.

Solar radiation is otherwise very dilute as it reaches the atmosphere of Earth and proceed towards the its surface. Optical concentration is an efficient way to increase the energy density of the radiation.

This allows the use of absorber/receivers with small surface area, with lower heat losses as losses are proportional to the absorber surface size. Again, high temperature may be obtained under **concentrated conditions**, and hence, as CSP and thermodynamics suggests conversion of solar energy into work may be done more efficiently at high temperature.

The concentrated solar energy must be converted into another useful form of energy, usually heat (hence the nomenclature *solar thermal*). If necessary, heat may be converted to electricity by use of a heat engine and generator.

CSP systems capture the direct beam component of solar radiation. Normal water (temperature 300 K) or a mixture of salt (preferably a mixture of NaNO_3 and KNO_3) at a given temperature can liquid. The liquids are pumped to the receiver of the CSP system. Receiver being already heated up to a high temperature, heats up this fluid and carries thermal energy with increase in temperature. This High temperature fluid is stored at the Hot Storage Tank (HST) and subsequently may be used for electricity generation using a turbine. The HST act as a thermal battery to store heat energy in the form of High Temperature Fluid and transfer it to the turbine as and when necessary.

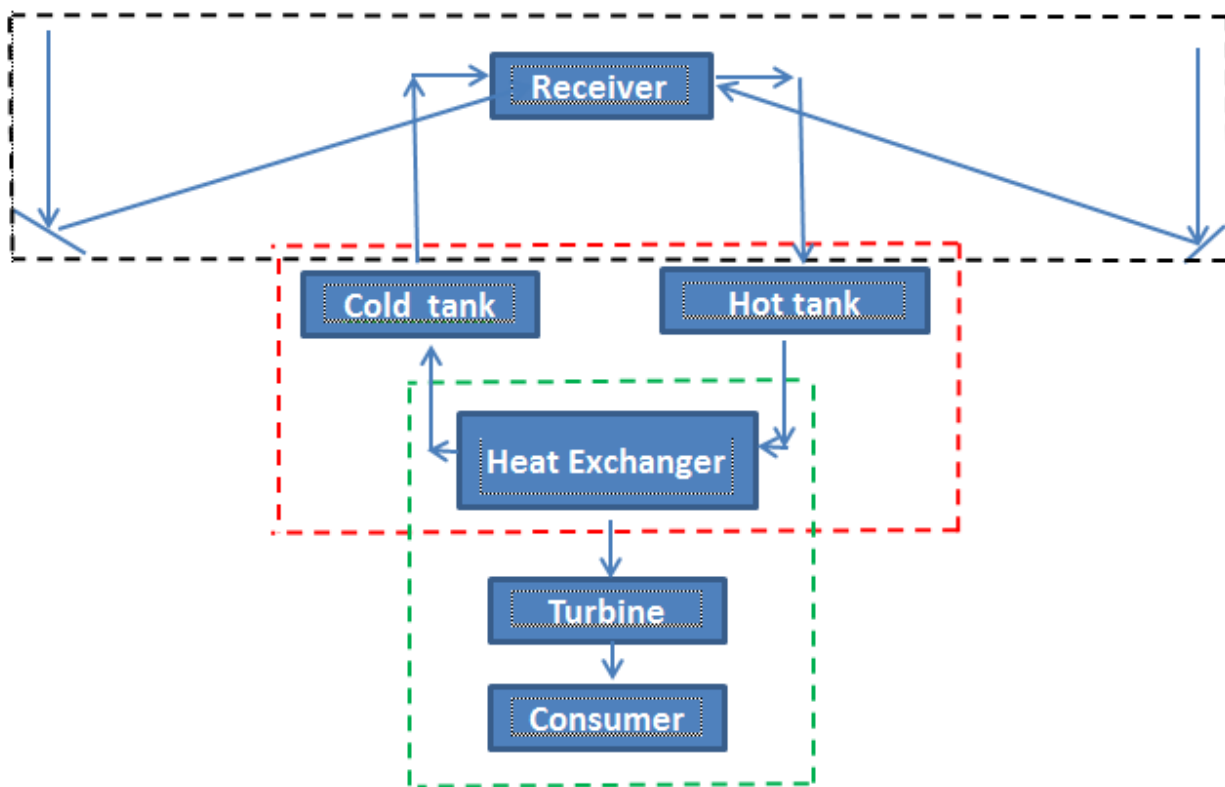


Fig 3.2: Skeleton of CSP

In figure 3.2, the basic engineering of the CSP is elaborated. The black box consists of the Heliostats on ground and Receiver at a calculated height, The Red box illustrates the heat exchange system. In this box, the heat exchanger perform dual task and a feedback loop system. One is to send the heat to the turbine and the second is to send the portion of the HTF which is not heated enough to the cold tank so that the heating continues. The green box collaborates with the working of the red box elements and demonstrates the passage of output of heat exchanger to the turbine for use in electricity generation (Consumer).

The various form of solar radiation concentration geometry may be categorized as below

3.2 Beam Up technology

For the beam-up technology of work, the heliostat field, as it is designed on the ground, is made to reflect the rays to an elevated tower.

3.2.1 Line focus technology

In this way of work, solar radiation is made to be incident on a linear absorber/receiver kept at a distance from the ground. The receiver is a one-dimensional fixed linear element of sufficient length and carry water/Heat Transfer Fluid. In broad scale, two different types of work are performed in this way which accepts radiation from the solar field and passes on the heat to its constituent.

3.2.1.1 Parabolic Trough (PT)



Fig 3.3: Parabolic troughs for solar collection [91]

Parabolic Trough [98,144] is a single axis sun tracking technology in which long rectangular reflectors are used to keep the Sun's focus on an linear absorber/receiver which contain a heat transfer fluid. First PT was installed in Cairo, Egypt in 1912.

In this technology, curved reflectors around one axis using a linear parabolic shaped mirror are used to collect rays from the solar beam to a line image upon reflection. The trough is usually aligned in the North South direction and rotated to track the Sun as it makes the diurnal movement across the sky

3.2.1.2 Linear Fresnel Reflector (LFR)



Fig 3.4 :Fresnel reflector for solar collection [99]

In the design of solar field using LFR, flat mirrors large in one direction and comparatively smaller in the other, are placed on the ground to reflect the input solar radiation to a linearly mounted element. As a convention, rows of highly reflective mirrors are kept on only one side of the linear absorber/receiver element.

As a variant of this design, Compact Linear Fresnel Reflector (CLFR) is used where multiple towers are used to significantly reduce the land usage. In this case, partial intermeshing between two single tower arrays is done which economics the land area required for the purpose. To achieve a fine focus on the receiver line, usually a curvature is used on the mirror [100].

3.2.2 Point focus technology

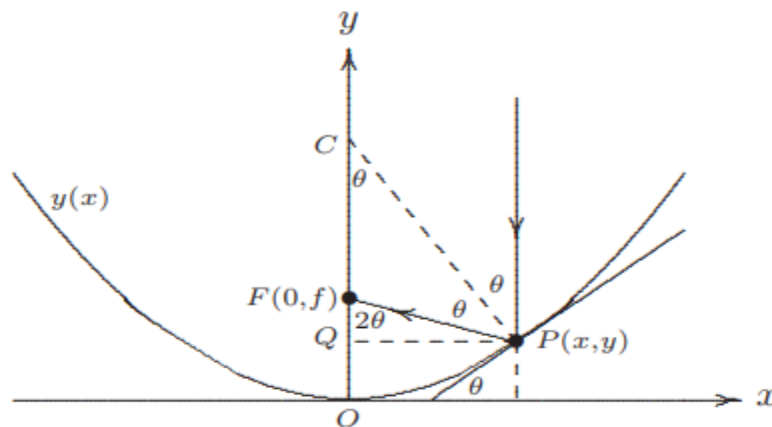


Fig 3.5 Conic section geometry

In point focus technology, highly reflective mirror, called Heliostats, are used to focus the incoming solar radiation to a point. Both spherical and Parabolic mirrors are used in these kind of setup. The Basic between these is that the parabola produces a perfect focus while sphere produce a fuzzy (blurred and spread) focal point [78]. Usually for these type of work, parabolic mirror are used (with conic constant of -1).For high concentration and to minimize the spot size on the receiver, curvature may be introduced. The mirror is part of a structure of radius r . C is the

center of the circle, since the line segment CP is perpendicular to the tangent line at point P. Hence the length of CP is equal to r. The triangle CFP is isosceles, hence the length of the sides FP and FC are equal. This length may be called a. Then using the law of cosines ,

$$\begin{aligned}
 r^2 &= 2a^2[1 - \cos(\pi - 2a)] \\
 r^2 &= 4a^2\cos^2\theta \\
 \text{or } a &= \frac{r}{2\cos\theta} \\
 \text{using } \cos 2\theta &= \cos^2\theta - \sin^2\theta = 2\cos^2\theta - 1 \\
 \text{Noting that } f + a &= r, \\
 f &= \left[1 - \frac{1}{2\cos\theta}\right]
 \end{aligned}$$

This last equation shows that there is no unique focal point, since f depends on the angle θ . However, if $\theta \ll 1$, then

$$\begin{aligned}
 \cos\theta &\cong 1 - \frac{1}{2}\theta^2 \cong 1 \\
 \theta \ll 1, f &\cong \frac{r}{2}
 \end{aligned} \tag{3.1}$$

3.2.2.1 Power Tower

In power tower solar collector, a field is generated with a set of highly reflective mirrors (Heliostats) on ground or little above. Solar radiation is incident on these Heliostats and gets reflected. In many cases, to avoid dusting effect, Heliostats are placed slightly above the ground. Proper two dimension tilt and curvature is given to the Heliostats for increase in solar radiation density.



Fig 3.6: Solar tower including Heliostat for solar collection [96,97]

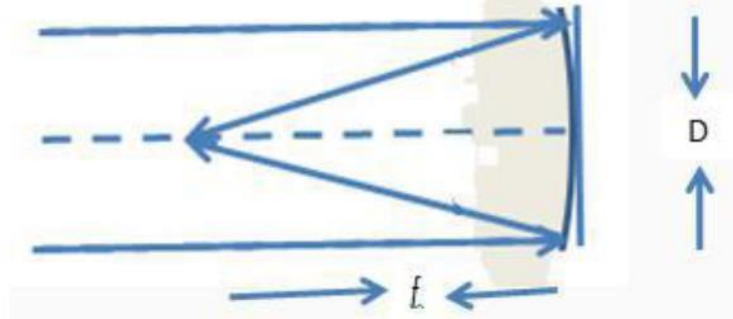


Fig 3.7: Curvature on the Heliostat

F number of Heliostat

F number signifies the light gathering capacity of the optical instrument. The surface of the Heliostat acts as the stop of the device setup. Considering Eq.3.2 the focal length, F number may be written as

$$F = \frac{f}{D} \quad (3.2)$$

F is a dimensionless number which quantifies depth of field of the image.

Numerical Aperture (NA) of Heliostat

The numerical aperture (NA) of an optical system is a dimensionless number that specifies the range of angles over which the system can accept light.

$$NA = n \sin \theta$$

For Heliostats (Considering aplanatic systems i.e coma and spherical aberration free) with infinite object distances, the F and NA are related as

$$F = \frac{1}{NA}$$

Considering index of work as one (1).

In **Power Tower** receivers, the temperature may reach more than 1000°C and thus allowing, as stated, high efficiency rates of energy conversion.

To increase the concentration at a small area, curvature and tilting of Heliostats is proposed.

3.2.2.2 Parabolic Dish-Engine

Solar dish/engine systems consist of two primary components

- a. The solar concentrator in dish form and
- b. The power conversion unit.

The solar concentrator in this pattern of work is a parabolic dish of highly reflective mirror which concentrate the solar rays directing to a thermal receiver which is located at the focal point of dish.

The power conversion unit usually consists of the thermal receiver and the conversion engine i.e a generator.



Fig 3.8 Parabolic dish and collector [100]

The thermal receiver, as mentioned, absorbs the concentrated solar energy in the form of rays and converts it to heat. Heat is then transferred to the engine/generator for further usage. A serious constraint in this manner of work is the limited size of the concentrator which is usually affected by wind motion. As a consequence of that, the power generated is accordingly limited.

3.3 Beam Down Optics

Literatures suggest the necessity of high temperature (~ 1200 K) on the receiver for increase in the efficiency of Solar thermal power generation. To attain such high concentrations at the receiver aperture, it is not considered sufficient to improve the performance factors of the primary concentrators as mentioned later in chapter 4. A secondary concentration, called BDO, is often recommended as an optical device which escalates the performance [101] of heliostatic power generation.

The secondary concentrator has its own inherent losses, which reduce the total optical efficiency. Also introducing the secondary concentrator has a negative effect on the optimal shape, size and arrangement over the primary concentrator.

In Beam - Down Optical (BDO) way of work for solar radiation collection, an additional optical element, may be called a Secondary reflector (SR), is used at an elevated height, and may be positioned above or below the conventional receiver position. The receiver in this case is placed at a convenient place, on or slightly above the ground. All the associated heat transport system was to be placed at/near the receiver position. The addition of SR leads to loss of efficiency of the field because of consideration of extra reflectance factor. However, this set-up has the advantage of cost reduction and better management of Heat transport system [102]. Together with that, the mechanical stress reduction is also an addition to better performance.

This model is based on the Cassegrain telescope design as in Fig 3.9. The model hybridizes this design with conventional Solar collection mechanism with receiver at top.

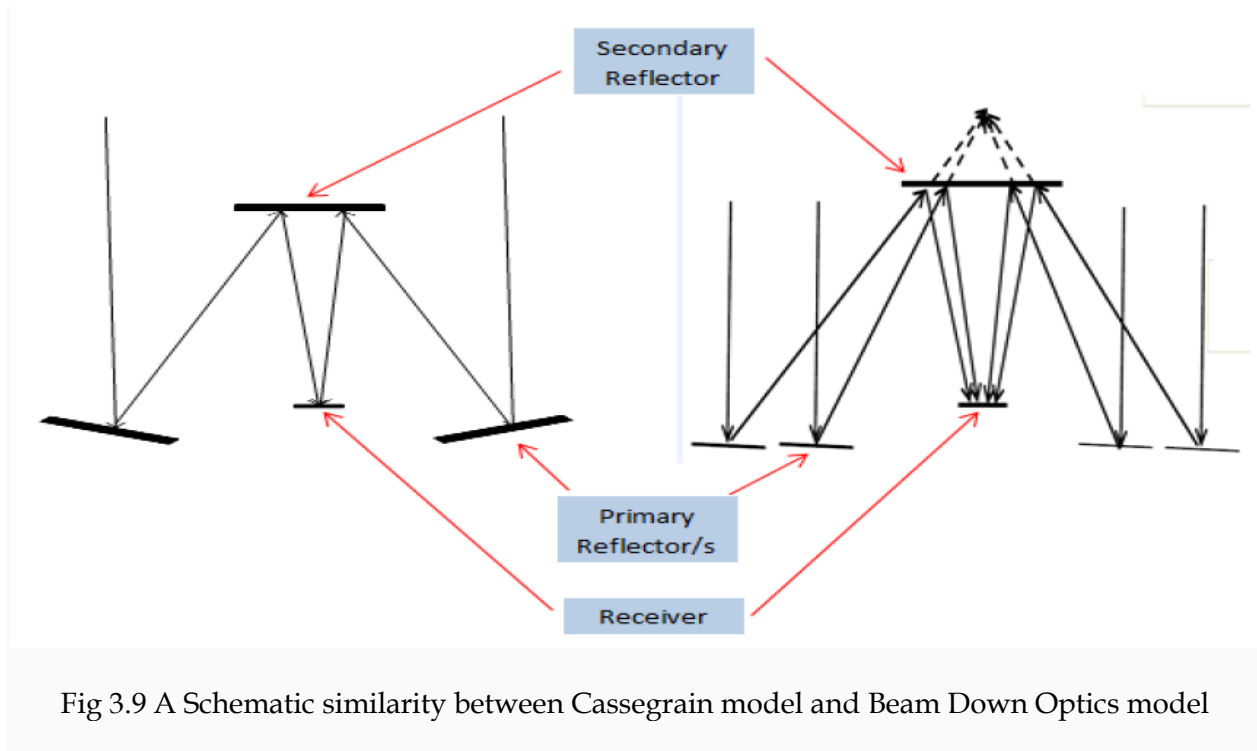


Fig 3.9 A Schematic similarity between Cassegrain model and Beam Down Optics model

As is evident from the name, the rays follow laws of reflection twice. Once on the Heliostat (Incident ray from the source and reflected ray towards the Secondary) and secondly on the secondary reflector (Incident ray from the SR and reflected ray towards the receiver). Shown in the Beam Down model in fig above [101,102], as the rays are targeted to the aim point, truncation of the path is done at a calculated height using the SR and the rays are directed to the receiver.

The truncation may be varied with multiple designs as mentioned below in subsections

3.3.1 Inclined Plane (IP)

In this setup the heliostats are laid on the ground and it reflects the radiation towards a receiver. As the radiation approaches the receiving point, its path is truncated by the inclined plane kept at a certain height. The plane is given a calculated angle which take the radiation to a point on the ground. The inclined plane is to be rotated one axis wise to make sure that radiation from the plane is incident on the receiver [103].

As the field consists of Heliostat spread at a considerable distance from the IP, it is necessary to expand the size of the plane to make sure that no ray is missed as they head towards a fixed receiver. As the size of the Plane increases, shadow effect and blocking of solar radiation by IP hampers the performance of rays placed at the first, second, or even later heliostats. To avoid this effect, it is proposed to ignore calculation from the heliostats which are actually blocked and introduce new Heliostats (if necessary) to compensate the number the Heliostats which are blocked.

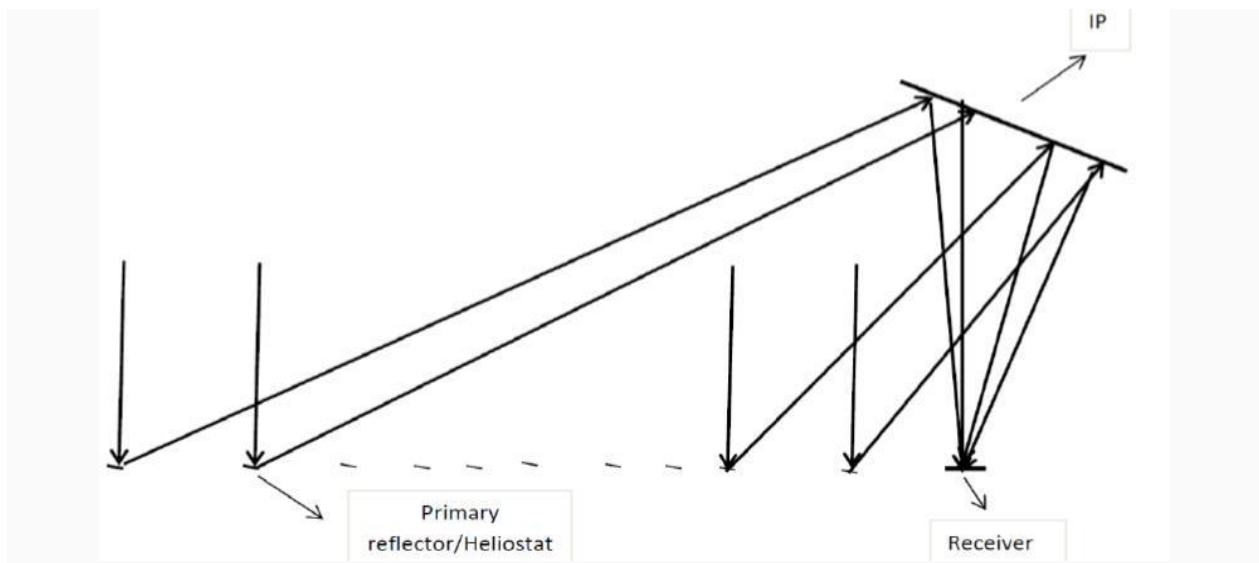


Fig 3.10 A Schematic diagram of the BDO with inclined plane

As the rays move from the Heliostats to the aim point, they obey **laws of reflection** and finally get incident on the receiver.

3.3.2 Conic section

Conic section geometry is used for Beam Down work utilizing the two foci structure. One of the foci is considered to be the aim point as mentioned below and the second foci is considered to be the receiver point on/near the ground. All conics satisfy Fermat's principle i.e they generate perfect imaging at two points. The conics serve the purpose of truncation at a height. Equation of a conic centered on the z-axis is given as

$$\rho^2 - 2Rz + (k + 1)z^2 = 0 \text{ where}$$

$$\rho = x^2 + y^2$$

R = Radius of curvature and
k = conic constant = - eccentricity²

As the conic section expands the bottom foci, it is proposed to use a Non-Imaging Optics component (Preferably Compound Parabolic Concentrator) above the receiver.

In the above case the heliostats were considered to be spread on the x-y plane on the ground.

3.3.3 Hyperboloid as secondary mirror

Hyperboloid is defined to be a geometric structure in which the focus (fixed point) and directrix (Fixed line) is constant [16,104].

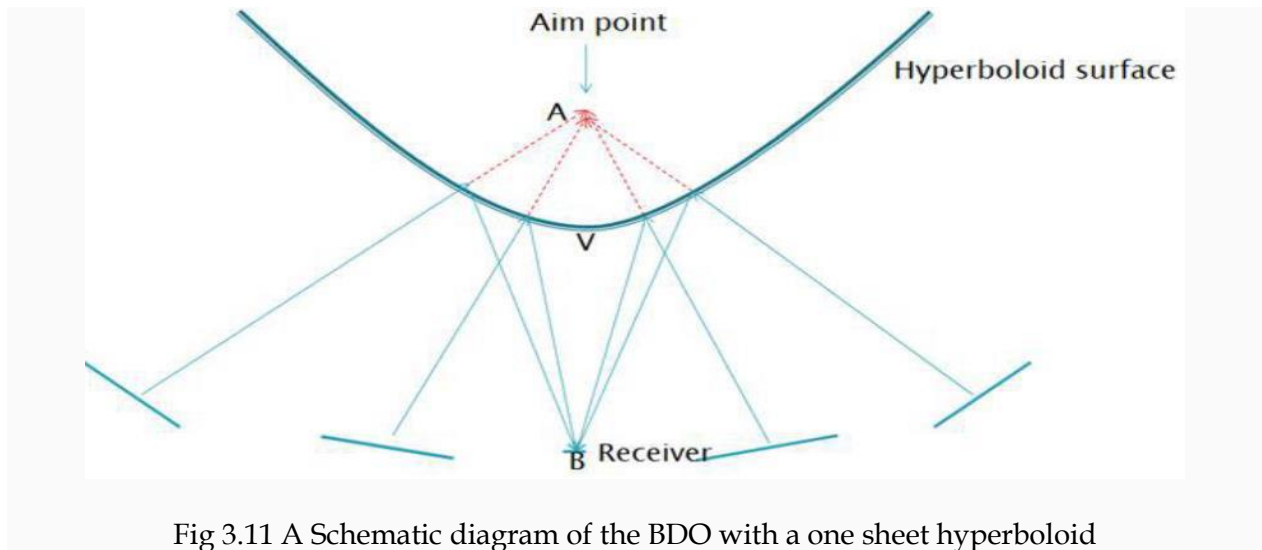


Fig 3.11 A Schematic diagram of the BDO with a one sheet hyperboloid

The above figure (Fig 3.11) show the foci (A) , Vertex (B). In this work, one sheeted hyperboloid was used and the second sheet as a material base was not necessary.

A hyperboloid reflector represents a convex mirror section whose convexity is used for the purpose.

The distance between two vertices is the major axis $2a$ and distance between co-vertices is the minor axis $2b$ in the figure.

The eccentricity of the structure may be quantified as

$$e = \sqrt{1 + \frac{b^2}{a^2}} \quad (3.3)$$

The focal length of the structure may be quantified as

$$f = \frac{a(e^2 - 1)}{e} \quad (3.4)$$

For this work purpose, as mentioned, a single leaf i.e upper leaf hyperboloid was used.

In Fig 3.11

AB is the optical / mechanical axis

The following are the necessary geometrical mentions [105]

V vertex

A Top focus (Aim point position)

B Bottom focus (Receiver position)

The distance $f_2 = VB$ is the bottom focal distance and

The distance $f_1 = AV$ is the top focal distance.

$$f_h = \frac{f_2}{f_1 + f_2} (3.5)$$

may be considered to be fractional position of the vertex of the hyperboloid from the height of the aim point [106] with the consideration of receiver point i.e the lower focal point and hence $0 < f_h < 1$. The magnification of the image is

$$M = \frac{f_2}{f_1} \quad (3.6)$$

General equation of one sheeted hyperbola

$$\frac{1}{x^2} + \frac{1}{y^2} - \frac{1}{z^2} = 1$$

$$c^2 = a^2 b^2$$

The foci are located at $(\pm c, 0)$

Distance between foci is $2c$

Vertex is located at $(\pm a, 0)$

Considering a standard hyperbola with x - axis coinciding with major axis.

3.3.4 Ellipsoid as secondary reflector

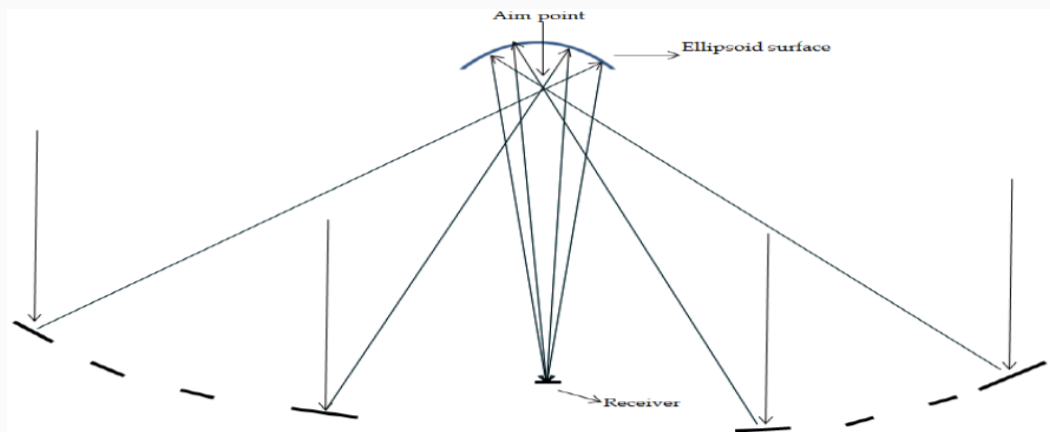


Fig 3.12 A Schematic diagram of the BDO with a one sheet ellipsoid

An ellipse, ellipsoid in 3d, may be considered to be a geometric structure with two (2) focal points. The focal points, together with eccentricity define the working. Eccentricity of this structure is between 0 (that of a sphere) and 1 (that of a parabola). This geometry, as in fig 3.12 presents two foci, one is considered to be the aim point in this work and the other is considered to be the receiver position [16,103,104]. In contrast to a hyperboloid, an ellipsoid reflector represents a concave mirror section whose concave surface nature is used for the purpose.

The fraction f_e as given below may be considered to be fractional position of the upper vertex of the ellipsoid from the aim point with the consideration of receiver point i.e the lower focal point

$$f_e = \frac{f_2}{f_2 - f_1} \quad (3.7)$$

The magnification happens rat the same rate as that of hyperboloid

The general equation of an ellipsoid is

$$\frac{1}{x^2} + \frac{1}{y^2} + \frac{1}{z^2} = 1 \quad (3.8)$$

3.3.5 Comparison between Hyperboloid and Ellipsoid as SR

1. The position of the hyperboloid mirror is lower than the ellipsoid [105]. This reduces the mechanical stress on the total design. It is observed that for equivalent efficiency, the height of the ellipsoid is to be kept at a double value than that of the hyperboloid together with larger size.
2. The identical optical behavior as achieved from hyperboloid would be expected with ellipsoid.

3.4 Optical field design

Solar field layout design is to locate the receiver with a calculated mirrors distance in a given land area. An efficient, economic and productive field design is the chief requirement of the work. The field design or a layout on the ground would mean placement of highly reflective mirrors on the ground which reflects the incident solar radiation in the form of rays directed to the recipient.

The recipient of that may be

- i) A Receiver placed at a height (Beam up) or
- ii) Another reflector (Beam down) called the secondary reflector.

In the second case, Radiation/ rays from the reflector at a height is directed to a receiver near/ on the ground.

As one of the biggest driving force of the energy costs (around 50 %) in the context of Solar thermal energy is the optical layout and consequently much effort is being made in the design of a low cost i.e more cost-effective heliostat field.

A perfectly flat Heliostat would produce an image on the receiver which would be approximately equal size of the heliostat with a Sunspread of 4.67 millirads ($\sim 0.3^\circ$).

The objective of work is to produce the minimum spot size. A major cause for the increase of the spot size as the radiation move from the Heliostats to the receiver is the Heliostat surface waviness. As canting is done on segmented mirrors in case of large Heliostats, the curvature of all the canted mirrors may not match. Other than these, there are errors mentioned in Chapter .All taken together, they produce a flux map on the receiver as shown in Fig 3.13 next page

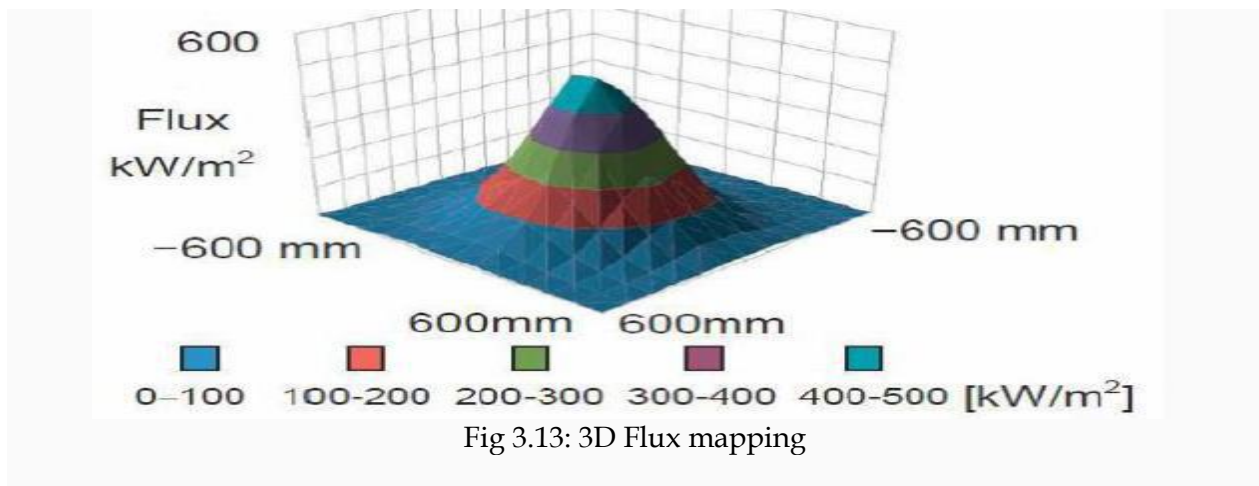


Fig 3.13: 3D Flux mapping

To avoid these effects it is proposed to introduce proper curvature on the Heliostats. Given below (section 3.5) are a set of practical and feasible setup of heliostats on the ground. In sub-section 3.9.3 the major manner of heliostat positions are elaborated and in sub-section 3.9.4 the sun tracking methodology is stated.

3.5 Spatial orientation of the Heliostat field

The basic objective of a feasible Heliostat field layout is

- To maximize the power output,
- To minimize the losses mention in section 3.8 and
- To maximize the usage of available land area.

3.5.1 Radial Staggered (RS)

Literatures suggest this method to be the most efficient and affluent for Solar Tower concentration. Getting its name from the radial network in the communication system i.e providing communication signals from substations to a station through wires connecting the nodes of a distributed system. Likewise, in Radial Staggered arrangement, the heliostats are placed as nodes in rows and columns as per Azimuthal spacing ΔA and Radial spacing ΔR so that that the losses, as mentioned in next section, are minimum [13, 106]. For this setup, Heliostats are arranged so that no Heliostat is an obstruction to any other, minimizing the blocking and shadowing effect. The distance between the rows in an alternate manner is called Radial spacing (ΔR) and the distance between columns in an alternate manner is called Azimuthal spacing (ΔA) as per the formulae in equation 3.9 and 3.10 next page

$$\Delta R = LM(1.44cot\gamma - 1.094 + 3.068\gamma - 1.1256\gamma) \quad (3.9)$$

$$\Delta A = WM(1.749 + 0.6396\gamma) + \left\{ \frac{0.2873}{\gamma - 0.04902} \right\} \quad (3.10)$$

$$\text{where } \gamma = \tan^{-1} \frac{1}{R}$$

R is the normalized distance of the first row from the tower foot measured in terms of tower height.

LM : Length of heliostat

WM: Width of heliostat

The first row is to be considered at a distance equal to the tower height or $\frac{3}{4}$ of the tower height [13]. The heliostat points throughout the field are calculated using ΔR and ΔA . That gives a section of a circle view plan-wise or the entire circle as it is spread on ground shown pictorially in figure-wise 3.14 below.

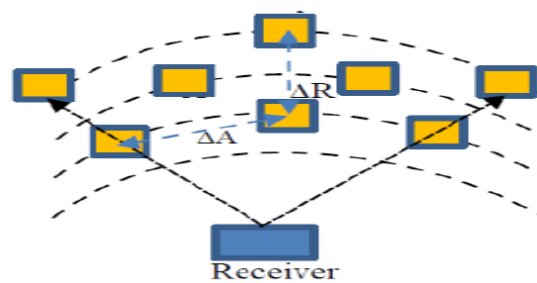


Fig 3.14: Radial Staggered Heliostat field setup [107]

As shown in fig 3.14, this arrangement has the benefit that no heliostat on ground is placed in front of another Heliostat in adjacent rings along a spoke to the tower. As a consequence, the reflected beam from the heliostats can pass between adjacent neighbors direct to the receiver without any disturbance.

The Heliostats at the solar field near the tower are considered to be most efficient for power generation. Although RS configuration reduces the shadowing and blocking effect, the transition of heliostat density from high to low density with distance from the tower is a disadvantage [108]

3.5.2 Cornfield

Cornfield design [109] (shown in Fig.3.15): In this configuration of field design, the Heliostats are spread on ground in a calculated manner as corns are spread for cultivation. The spacing between the rows and columns was done according to the dimension of the heliostat and chosen separation to minimize losses. In this biometric setup (in Fig 3.15), Heliostats are arranged in row and column wise in a manner corns are put on the field for plantation, minimizing the possible losses.

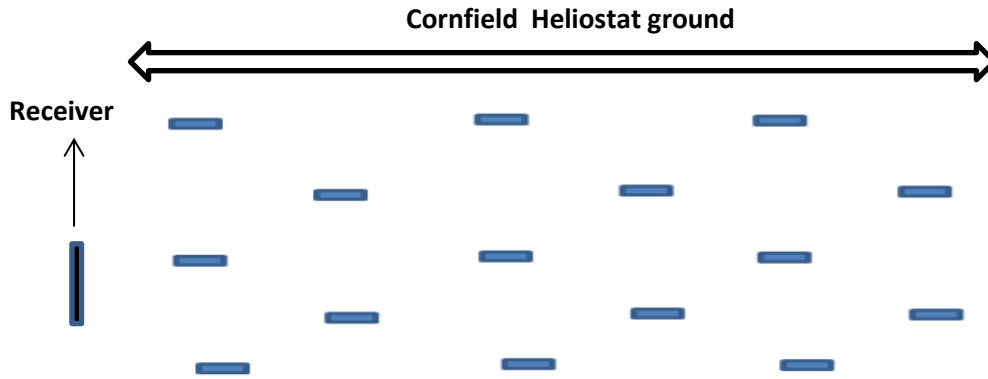


Fig 3.15: Cornfield Heliostat field setup

The Characteristics Diameter d_m of the setup is defined as the distance between the centers of the Heliostats in the next row/column

$$D_m = \sqrt{l^2 + b^2} + d \quad 3.11$$

where l and b are respectively the length and breadth of the heliostats and d_s being the required distance between the rows/columns. D_m is the characteristic diameter of the setup.

3.5.3 Sunflower

This biometric manner of field design follows the Fermat's spiral pattern with the following calculation.

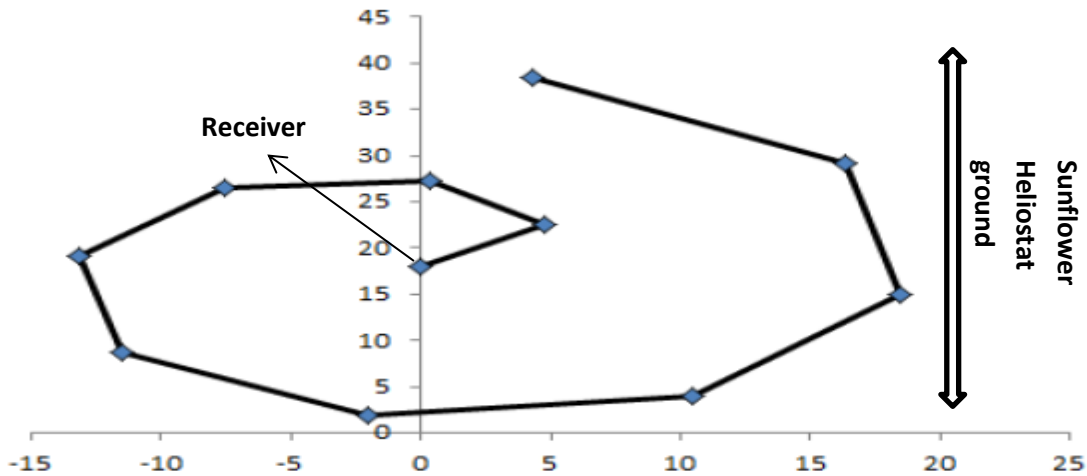


Fig 3.16: Heliostat field set for Sunflower field as symbolic dots

The Fermat's Spiral algorithm presented in [110, 111] generates heliostat field based on spirals, as they have a continuous density function representing the spirals as found in a Sunflower. The position of a heliostat is defined as

$$\theta_k = 2\pi\varphi^{-2}k \quad (3.12)$$

(where φ is the golden angle of the spiral design defined as $137.5^\circ / 2.4$ rads, k signifies which Heliostat in the field) for the angular position and

$$r_k = ak^b \quad (3.13)$$

for the radial position.

As in the above equation, use of this layout has two pre-requisite

1. A power Fermat's spiral parameter (a) and
2. The Heliostat dimensions (b).

a and b in Eq 6.5 are usually calculated on the basis of Radial Staggered design.

Together this, the following paraphernalic points are relevant.

1. A buffer distance between the active heliostats on the field.
 2. A minimum heliostat radial distance between the tower and the heliostats so that the spiral is not disturbed and
 3. The total number of heliostats in the field.
- are necessary input parameters.

In the Fig 3.16, central mark as shown, is the positions of the elevated receiver.

3.6 Receiver

Receiver is that part of this design system which determines the number of rays intercepted from the collector (Heliostats). Consequently it establishes the flux incident, temperature and power generated. For that reason, various forms of receiver designs were simulated, implemented and in many a case comparative studies were done.

3.6.1 Flat Receiver

In tower top CSP arrangement, the flat receiver is placed at a calculated height atop an installed tower. It has thermal installation and financial advantages but suffers from the disadvantage of heavy spillage losses. As the optical quotient of rays from Collector to Receive continuously suffers from Astigmatism, the size of the receiver has to be larger than the Heliostat size (in case of flat Heliostat).

3.6.2 Cavity Receiver

Concentrated solar energy is utilized for the use of solar thermochemical source of process heat generation for driving high temperature endothermic engines and, consequently storing energy in the form of transportable chemical fuels [112, 113].

Solar thermal applications in this regard usually feature the use of a cavity-type configuration which is supposed to have an enclosure designed to effectively and efficiently capture incident solar radiation entering through a small opening. Larger the ratio of cavity area to the aperture area, the closer the cavity-receiver combination approach a blackbody absorber. However, higher conductive losses happen through the insulated cavity walls. To achieve an optimum aperture size of cavity device, a compromise is sorted between maximizing radiation capture and minimizing radiation losses[114].

Cavity receivers, designed in various forms, are well accepted for their ability to attain high efficiency, both in terms of geometric concentration and also power achieved and thereby they are used for solar radiation concentration into high thermal energy in a working fluid. The cavity shape, buoyancy wise air-trapping within the cavity effects usually lead to this high efficiency. In this connection, the light-trapping capacity arising from the cavity size and shape also reduce the convective losses from hot internal surfaces, and thus reduces thermal emission losses from the system [115].

Integrated models of receiver for heat transfer have been designed for a range of cavity receiver systems. Spindler et al [115] produced possibly the earliest of these models which consisted of an air receiver, with solar and thermal radiation modelled, but it had no external convection. Shuai et al studied the shape of cavity receivers with a hard-edged aperture and suggested a pear-shaped receiver cavity. It had the benefit of uniform flux inside the cavity[116]. In recent times, powerful numerical modelling has enabled an integrated set of optical/convective/radiative modelling of various receivers with detailed computation fluid dynamics (CFD) simulation of convective losses [117].

Solar thermal concentration with cavity receiver presents a non-isothermal receiver with an aperture absorbing surface for the low-flux regions of the focal plane which may be optimized to achieve maximum receiver efficiency through consideration of various losses and hence optimizes the exergetic i.e high energy conversion of the incident flux profile.

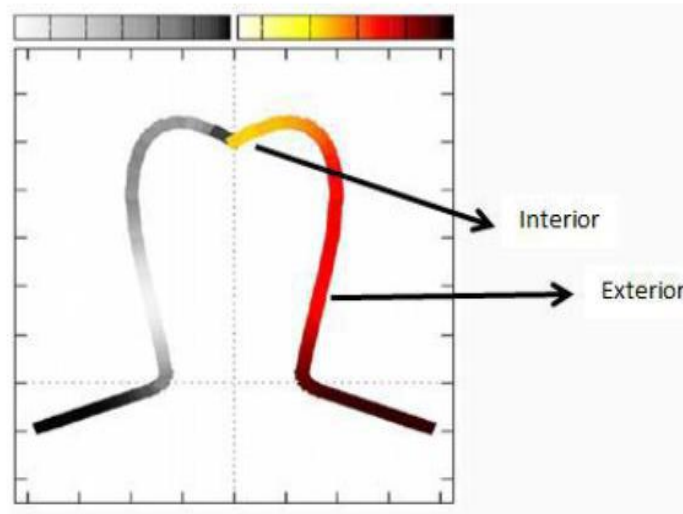


Fig 3.17 : Proposed cavity receiver with cross-sectional flux profile

In the above figure, rays from the first and second rows of heliostats (27), get incident on the interior surface and the rest (i.e 154) are spread on the ground in seven rings. The spread (for both the set as mentioned) was done in a Radial Staggered pattern as mentioned in Eq. The performance of the cavity receiver mentioned includes optical modelling, emission, convection, conduction, and hydrodynamic models in an integrated manner. The optical model in this set is independent of the temperature of the walls of the cavity. Other than that, all the mentioned models involve the calculation of the associated heat transfer [117]. The use of integrated cavity receiver i.e the heat transfer model as described would make it possible to generate an iterative design process which would make a wide range of cavity receiver geometries to be considered.

The probabilistic optimization and manual process, as mentioned, was usually used to identify the best-performing configurations, to incorporate a range of design considerations. Instead of a straight forward way to include in the model, adjustments were proposed as per necessary requirements. Some of those were as follows

- a. Standard size of the tubular portion
- b. To minimize spillage, diameter and cone- angle of the circum-aperture region.
- c. Increase the lower-side pipe dimension.
- d. Internal cavity walls to push the outer regions beyond the high flux part.
- e. Smooth cross-sectional profile near the main cavity part to provide smooth transition between the circumcenter to the cavity.
- f. To achieve more uniform flux, cross-section profile is to be kept smooth [118].
- g. Optical effects of cavity material.

Fig shows the optical design of this model but the to make the device workable in an efficient manner, it is necessary to take in consideration the following supporting models

a. Thermal emission loss model:

This refers to the re-radiation of emission from the figure leading to reduction in concentration. A conical section is used at the back of the receiver covering the part where the structure curvature would exceed certain limits and modelled as an adiabatic wall.

b. External Model to nullify convective loss:

As a major shift from non-cavity receivers, in case of cavity receivers, convective loss is a major focus in the analysis. In fact convection losses are equivalent to radiative losses in magnitude calculation. However for cavity receivers without a window, convective losses usually dominate the design.

c. Hydrodynamic Model.

The flow path of radiation in this model was divided into segments approximately with one flow segment for each complete loop of receiver model. For this purpose, the radiation flow through the cavity receiver was designed using a steady-state model with one-dimensional finite-difference fluid flow, keeping mass, energy and momentum balances into consideration.

d. Conduction Model.

This is a thermal resistance model which is calculated for the insulation purpose. Other than this, as the receiver is surrounded with cladding, this model acts as a protective layer

For successful working, all the four models mentioned had to be integrated with the optical model. The device is designed to receive the solar radiation as an input which raises the temperature. Optical model is not temperature dependent but the rest models are. The hydrodynamic model is one dimensional and the rest are mostly two dimensional. For adjustment of these models, binning of the cavity between four models, analyzed separately, is to be aligned so that one dimensional flow of radiation in the hydrodynamical model corresponds to frustum shaped area having the same axial displacement as the centerline of the pipe helix.

3.6.3 Bladed receiver

Conventional flat receiver accepts the heat from Sun (through Heliostats) and thereby transfers the heat to fluid which absorbs the heat as it is made to flow through the receiver.

In this way of design, limitations on peak fluid temperature, mechanical stress on the receiver together with radiative losses couple amounting into constrained peak flux accumulation. That, in turn, limits the efficiency of receiver [119].

An approach to improve the mentioned setup and increase receiver efficiency is mentioned in literature to reconfigure the flat plate into 'bladed structures where a parallel set of multiple flat plates

are arranged in bladed structure. The bladed structures have the capacity to improve light-trapping ability with compressed radiation into a smaller aperture area and that opens up a way to increase the flux incident on the aperture without exceeding the peak flux limitation.

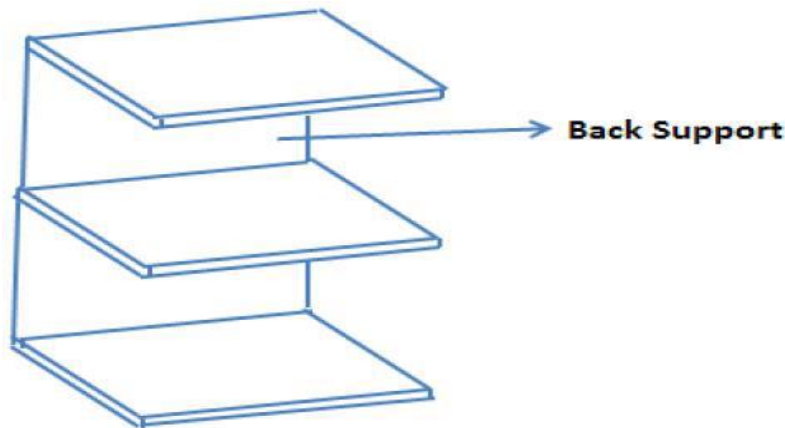


Fig 3.18:Bladed receiver with three blades and the back support

Heliostat field layout affects the optical efficiency and the flux distribution uniformity of a set of bladed receiver chiefly the blade concentration and position of the blades. To increase the efficiency, it is proposed to introduce a calculated angle of the individual receiver. As a back to the receiver set, a wall is installed which together with being a support also takes care of the spillage loss factor. This way of work become important when instead of curved and Heliostat flat Heliostats are used when becomes a important loss especially large fields. Usually multiple iterations are necessary to optimize the number of blades to be installed.

3.6.4 Cylindrical receiver

This receiver has the characteristic of receiving rays from all quadrants of the field. That makes it efficient in intercepting rays when the field is circular/spiral. For that reason, it was used in this work when the field was spiral.

3.7 Angular orientation of the Heliostat

The angular orientation i.e the sun-tracking mechanism is aimed at tilting the Heliostat in a manner so that the rays hit the receiver. The widely implemented mechanisms are discussed in sub-section 3.7.1 and 3.7.2

3.7.1 Azimuth - Elevation (AE) method

In this method, one of the tracking axes of the heliostat, the center point towards the top i.e the zenith point and the other axis is perpendicular to the first axis and hence, tangent to the heliostat frame [120].

3.7.2 Spinning - Elevation (SE) method

In this setup, one of the tracking axes of the heliostat point towards the target (receiver) , the spinning axis, in order to maintain the normal to heliostat and the second axis is perpendicular to the first one and also tangent to the heliostat frame in order to adjust the heliostat normal until it bisects the sun position vector and the receiver position vector.

As the positions of the sun and the receiver are permanent and independent of the sun-tracking mechanism, the only difference between AE and SE lie in the utilization of difference to rotate the heliostat frame in order to achieve same incident angle but different orientation so that both can separately aim the sunlight towards the receiver.

3.8 Losses involved and aberrations in the Optical field

Solar field design, being consisted of optical elements, suffers from two categories of disturbance or losses i.e namely

3.8.1 Related to Solar field

Solar field being exposed to open atmosphere suffer from multiple losses which reduces the concentration capacity of the field and also mechanism to carry the radiation from field to the receiver and its storage. Some of the relevant losses are listed below

3.8.1.1 Shadowing

Shadowing refers to the hindrance that radiation vector from Sun face as it moves towards the heliostat. Any heliostat in the path of the vector connecting the solar point and the Heliostat point cause this effect.

The performance of any solar Heliostatic field is a function of layout on the field which to a large extent is further dependent on Degrees of Freedom (DOF) involved as mentioned below

- a. Size of the Heliostat plays a definite role in the power generation and the size of the field layout.
- b. As the beam flux accepted and reflected by the smaller Heliostat is usually lower than the larger, it is proposed to place small Heliostats on ground. To keep the power level generated as constant, multi-towered field may be implanted.
- c. A region surrounding the tower is to be kept free of Heliostats. If need be, the compensation in number of Heliostat may be done at the back of the calculated number of Heliostats. Paraphernalic equipment e.g pumps, heat exchangers and turbines for generation of power are usually spaced near the tower.
- d. Tower and receiver size play an important role in shadow loss on ground.
- e. Together with 4 above, receiver play an important part in concentration of the radiation from ground and temperature attained [105,121,67,16,109,122].

As the entire work is based on geocentric theory of Earth Sun relation, and the Sun is considered to rotate and revolve on the sky according to θ and ϕ (as mentioned above), all losses of the field vary according to the diurnal and annular motion of the Sun

Optical efficiency is considered to have a direct relation with the energy that hits the collectors, i.e. Heliostats in this case, and the receiver atop the tower. Total available solar energy on the receiver improves this efficiency and depending on that the size of the solar field is set. As design of solar field bears a high quotient of the total cost of the expense on the plant, an optimized field setup is related directly to the reduction of cost [123].

In Solar thermal optical setup for generation of renewable energy, as mentioned, central solar power tower takes a prime position. As mentioned in chapter 2, Heliostats follow the solar motion (as per changes in altitude and azimuth angle) and reflect the input sunlight to a receiver located at the tower top and the design on the field play a key role in contributing to the performance and contributes on the aspect of total cost of power plants [124]. The Elevation and Azimuth angle of the Sun on ground, as mentioned in chapter, generates the shadow coordinates on the ground and may be considered as one of the most practiced pattern [125].

Two of the most important losses that solar field face is because of the **Shadowing** and **Blocking** effect on the field design. The position with maximum possible efficiency is not stationary, but varies with solar position. So conventional stationary heliostat fields were placed in such a manner as to achieve the best efficiency integrated average over the year.

To attain that, it is necessary to calculate and accordingly minimize the space which is to be kept vacant for shadowing and blocking effects. The field is to be designed in such a manner that the proper spacing is kept in the design.

The top coordinates of the shadow with the pole as origin of a vertical pole OP

$$x = OP \frac{\sin(\Phi-180)}{\tan \theta_1} \quad (3.14)$$

$$y = OP \frac{\cos(\Phi-180)}{\tan \theta_1} \quad (3.15)$$

Φ and θ_1 indicate angles as in Eq 2.5 and 2.6

In the design, the heliostat shape is to be considered. Likewise, as rectangular heliostat is generally used, both the sides of the heliostat is to be considered. That would generate rectangular shadow effect on ground.

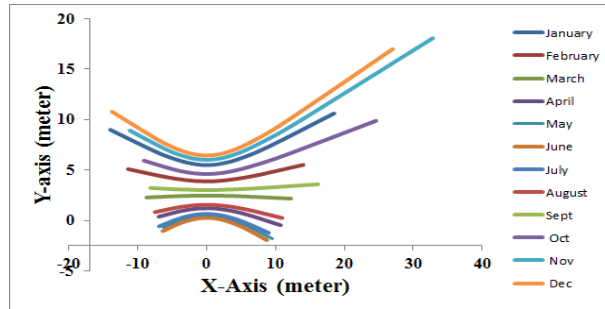


Fig 3.19: Shadow mapping

The Heliostats in this work was taken to be as rectangular (square) which make the shadow on ground to be trapezoidal. As the position of sun varies throughout the day, the shape of the trapezoid changes from being a perfect trapezoid at morning and evening (due to low sun angles) to thick straight line during noon.

The size of the shadow on the ground influence the spacing of heliostats and accordingly the field pattern is determined. Considering the breadth of the heliostat on the ground being AB and the height being AC and BD respectively where

$$A \rightarrow (x_1, y_1), B \rightarrow (x_2, y_2), C \rightarrow (x_3, y_3), D \rightarrow (x_4, y_4)$$

the size of the shadow i.e the trapezium on ground, in terms of a quadrilateral is [51]

$$Area = (x_1y_2) + (x_2y_3) + (x_3y_4) + (x_4y_1) - (x_2y_1) - (x_3y_2) - (x_4y_3) - (x_1y_4)$$

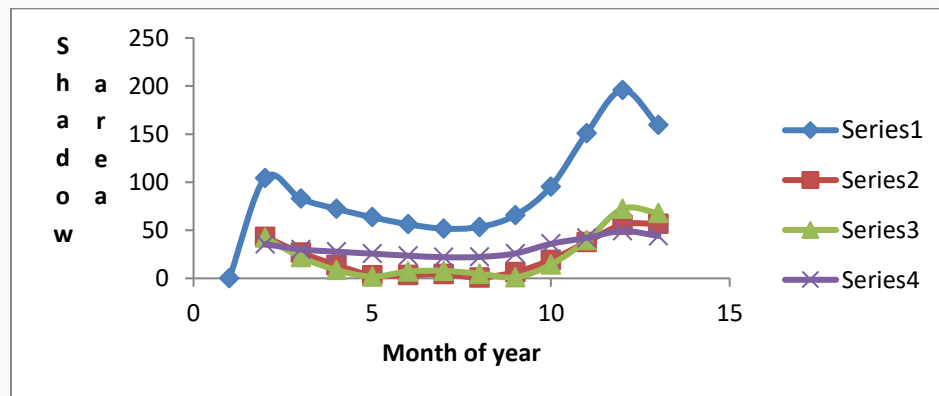


Fig 3.20: Shadow area on ground

The above shadow diagram is a manifestation of shadow coordinates together with heliostats bottom coordinates.

The shadow area diagram shows November shadow to be the most space occupying and thus most loss making month in this term.

Any optical system, irrespective of imaging behavior and purpose of use, is every time subjected to multiple aberration/s. In solar thermal work, this refers to the incapacity of the

imaging/nonimaging optical devices to form the perfect Sunshape on the receiver. Use of ray tracing manner of solar concentration and consequent power generation , the rays are to be considered as marginal i.e off-axis. Accordingly, the following aberrations are relevant in the process.

3.8.1.2 Blocking (η_B)

The figure (Fig. 3.21) next page is an elaboration of a) and b)

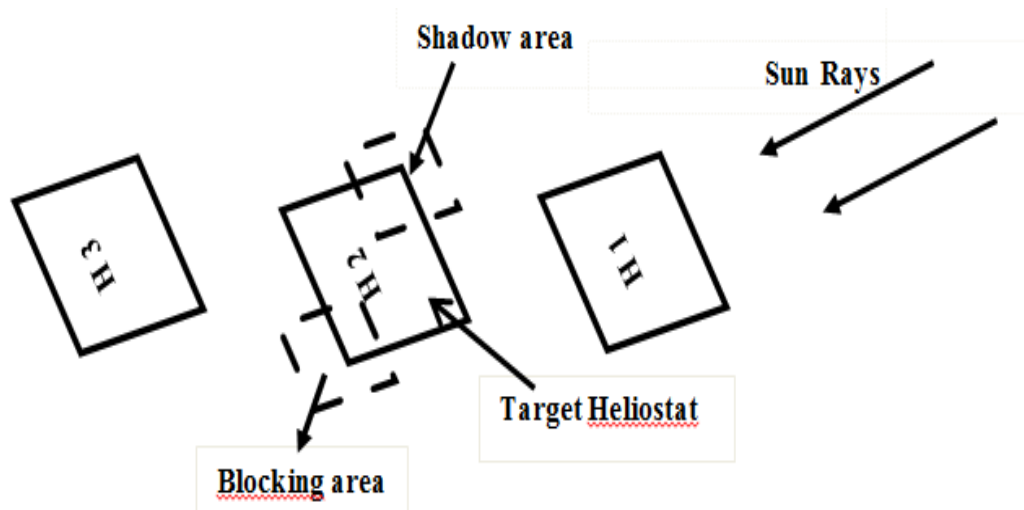


Fig 3.21 : Shadowing and blocking effect

Heliostat H_2 may be considered to be a test object. As the solar rays approach H_2 , it strikes the heliostat H_1 prior and lead to a blocking effect of the rays on they proceed to hit heliostat H_2 .Thats lead to **Blocking** effect on H_1

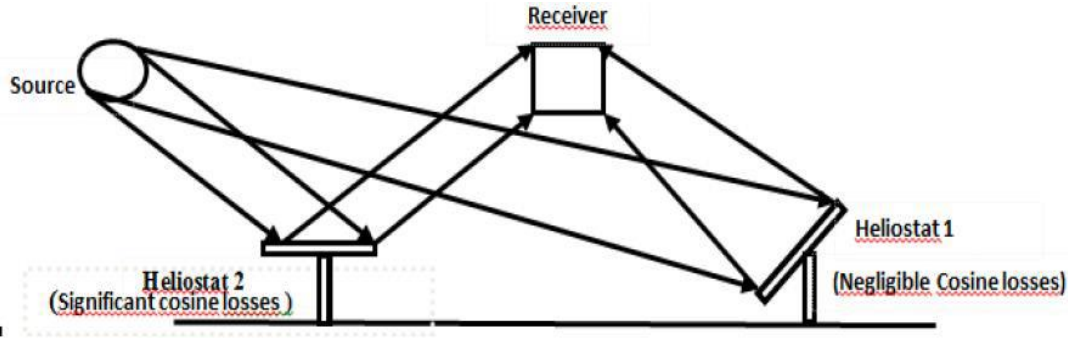
Blocking refer to the blockage of solar radiation from a heliostat to the receiver because of a neighboring Heliostat. Radiation from any heliostat , except the side or in the first row suffers from blockage due to three heliostats. Two in front on either side is called 'Shoulders' and the third i.e in front of the same column is called the 'Nose'. Blocking refers to the disturbance in the connecting vector between the Heliostat and the receiver.

As the rays hit H_2 , they cast a shadow of H_2 on the Heliostats H_3 which may be a considered a loss of effective space of radiation on H_2 .That leads to **Shadowing** effect on H_1

3.8.1.3 Cosine factor (η_F)

Cosine factor come into play as cosine of the half angle between two lines i.e

- i) Vector A connecting the Sun to the Heliostat H_2
- ii) Vector B connecting the heliostat H_2 to the receiver



$$\cos 2\theta = \frac{\vec{A} \cdot \vec{B}}{AB}$$

Fig 3.22 : Cosine effect [126]

As the considered field is consisted of multiple Heliostats, the position-wise spread of radiation lead to this loss. Tilting is to introduced 2d-wise to assure that Sun shape on the receiver replicates that on the Heliostat. As in Fig 3.22 , Heliostat 2 is not tilted any ways which lead to this loss. Heliostat 1 is tilted as mentioned. Likewise, all the Heliostats are tilted based on Heliostat position and hourly Sun position.

3.8.1.4 Reflectance (η_R)

As the rays are traced from the solar point to heliostat points, they are reflected following laws of reflection to the receiver. The material on the Heliostat surface coating usually has a reflectance less than 1.

3.8.1.5 Atmospheric attenuation (η_A)

The radiation, as it traverses from the heliostats to the receiver, passes through the atmosphere which introduces losses due to scattering (Rayleigh and Mie) and also absorption. The loss depends on the distance between the heliostat and the receiver d_h and also on the weather i.e visibility of the day considered.

$$\eta_A = 0.99321 - \{(1.176 * 10^{-4}) * d_h\} + \{(1.97 * 10^{-8}) * d_h^2\} \text{ when } d_h \leq 1000 \text{ m}$$

$$\text{and, otherwise, } \eta_A = e^{\{-0.0001106 * d_h\}}$$

As the distance of the heliostats increases from the tower i.e the field size increases ,the interception factor decreases and hence η_A decreases

In many of the cases, the performance of the layout depends on the operating hours of the day and the time of the year. Especially, the shadow effect becomes one of the biggest loss factors on many occasions, especially during morning and evening times when the solar angles are low. .

The total loss may be written mathematically as [127]

$$\eta = \eta_B \eta_S \eta_C \eta_R \eta_A \quad (3.16)$$

Although the above losses are considered to be prime that disturb the setup orientation and performance, other losses that affect the ideal solar imaging are as follows

1. Canting Errors: As mentioned, large size heliostats lead to heavy beam magnification. To reduce that effect, large Heliostats are made with multiple smaller heliostats canted together to give a structure. The imperfect joining and primarily the curvature mismatch i.e non - coincidence of focal point on the receiver from individual facets is the source for this error.
2. Optical errors: These errors rise because of surface imperfections and may be combined as a sum of roughness (microscopic) and sloppiness (macroscopic). These surface imperfections are resultant of several hills and valleys.
3. Geometrical errors: This generates because of factors like placement of Heliostats and its tracking of the sun, Heliostat 2d tilting to focus the radiation on the receiver.
4. Curvature errors on the heliostats: The mirror surfaces are nor perfect and suffer from minor waviness which may cause spillage and other effects.
5. Spillage (η_{sp}): This happen because of finite size of the receiver. As the size of the field i.e as the number of Heliostats on the field increase, the interception of radiation by the receiver go down i.e spillage of radiation increases. For this reason the size of the receiver is kept as equal (if felt necessary marginally bigger) to the size of the furthest heliostat as the divergence of radiation for it would be the maximum.
6. Air Mass (A_m): Air mass may be considered as a loss factor which depends on volume of air that the solar radiation needs to travel through atmosphere before it can be considered for insolation at collector on ground. Mathematically, it is the cosine of the solar zenith angle and hence as the distance between the point of insolation and the point directly under the Sun changes, A_m changes.[127,128]

As a consequence to the above errors summed up, the sun shape on the receiver is not an exact replica of the solar image that is seen on the sky. The concentration ratio also, because the receiver size is to be increased, decreases.

Although negation of the above is desired, but due to the transit movement of Sun and other geographic factors, the position of the Heliostats on the field with maximum efficiency is not stationary. Due to this behavior of the setup of work, an average efficiency over a long time is considered.

3.8.2 Related to Optical field

Apart from those mentioned in section 3.8.1, the optical components of the field suffer from other aberration as mentioned below in section 3.8.2

3.8.2.1 Spherical Aberration

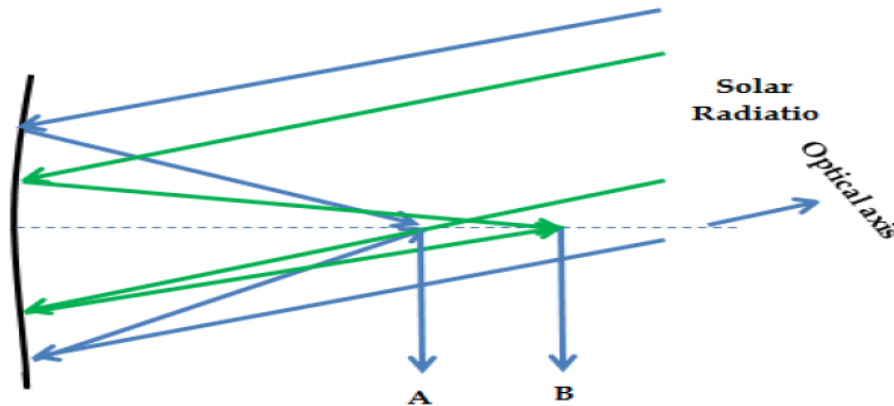


Fig 3.23 : Spherical Aberration

Fig 3.23 is a pictorial view of Spherical Aberration which is caused because of failure of the Heliostat i.e mirror to reflect all the incident rays to a single focal spot [78, 129]. While the rays which are close to center of optical axis of device are taken to focus at a further spot B, rays which are further away from center are taken to focus at a nearer spot A. This causes a spread in the focal spot on the receiver.

3.8.2.2 Coma

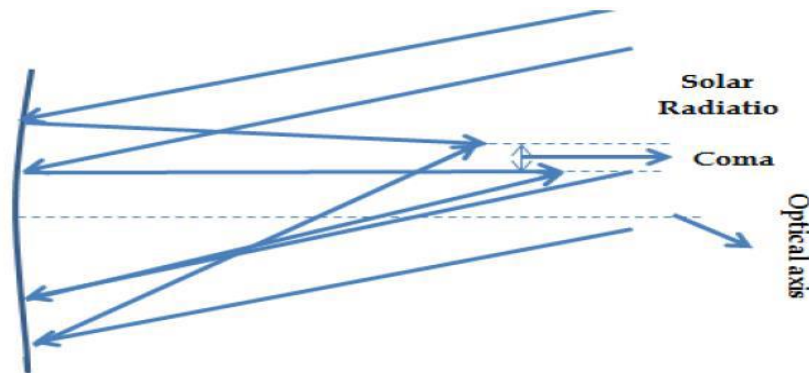


Fig 3.24: Coma

Fig 3.24 is a pictorial view of Coma as it is defined as variation of magnification with aperture position where the incidence of rays happens. As the incidence of rays for Solar collection is a set/bundle of oblique rays on the mirror, the rays passing through the side portions of the lens

are imaged at a different height as compared to those passing through the central portion. This distance between the positions of focus is referred to as Coma.

3.8.2.3 Distortion

In case of an off-axis object point, which is very common in Solar work, the image point is formed further away or closer to the expected calculated height of the image on the receiver in both the direction, horizontal and vertical. This is referred to as **Distortion** of image of an extended object as in Fig below.

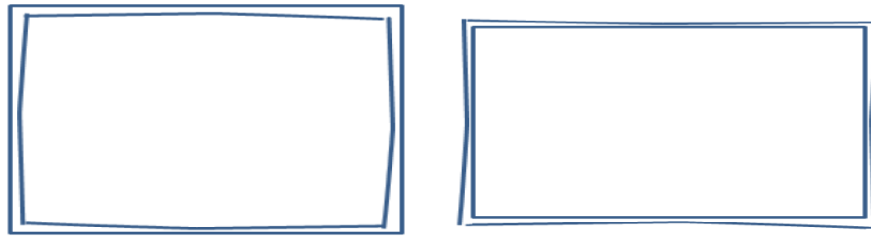


Fig3.25 Distortion in two form a) Barrel Shaped (left) and b) Pin Cushion(right)

As shown the figure, both the type of distortion disturbs the actual size of the image. In case of Pin Cushion the dimensional size of the image is reduced and in case of Barrel Shaped, the dimensional size is increased.

3.8.2.4 Optical Astigmatism

Chief ray is the ray which passes through the center of curvature of an optical system and moves in an undeviated manner. As a special property, upon reflection, it passes through the same path. The plane in the optical system which contain the Chief ray and the Optical axis is called the Tangential plane. The plane containing the chief ray and perpendicular to the tangential plane is the Sagittal plane.

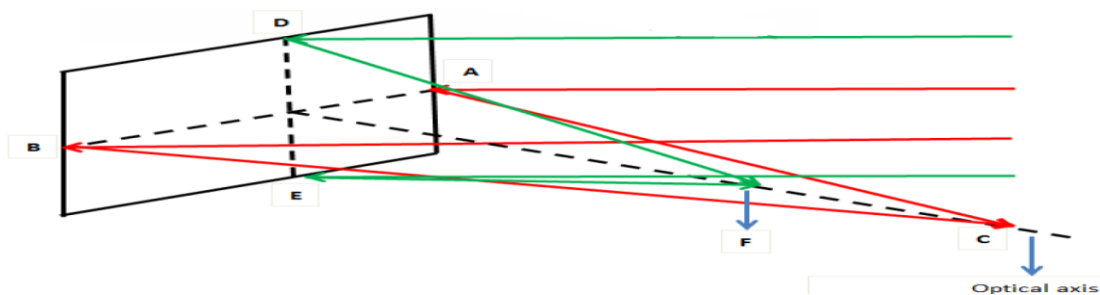


Fig3.26 : Astigmatic aberration

The above Fig is a pictorial representation of optical astigmatism. In fig 3.26, the red coloured triangle i.e ABC is called the Tangential plane on the image picture and consequently C is called the tangential focus. As a perpendicular to this, the triangle made by DEF is called the Sagittal plane and F is the sagittal focus. In an ideal condition, these two triangles must coalesce and foci

must be one. But, as the solar radiation is highly off-axis and because of the distance it traverses through the atmosphere, following Huygens's principle, the divergence increases and that causes severe astigmatism.

For solar concentration, astigmatism gives rise to spillage as described in chapter.

3.8.2.5 Curvature of field

Petzval Curvature, as a function of index of the material and the geometric curvature of, is connected with every optical element. Fig below shows Curvature error of optical system.

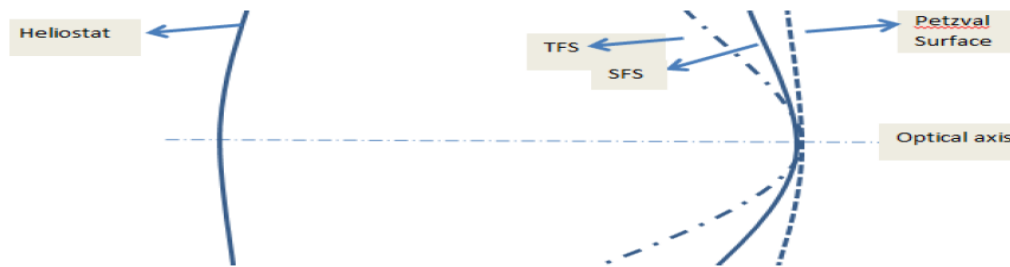


Fig 3.27 : Curvature of field aberration

In astigmatism-free mirrors, the tangential and sagittal plane ideally coincides and they lie in Petzval surface. In case of astigmatic mirrors, the tangential (image) surface is thrice the distance of the Petzval surface with respect to sagittal image. In either case, both the image surfaces are on the same side of the Petzval surface,

3.8.3 Related to Reflector surface

During operation of the field, the Heliostats i.e the reflective surface material is exposed to climatic stress factors which cause degradation and which changes throughout the year [130-132]. The direction component of Solar radiation, as it moves from the Heliostat to the Receiver, is one of the most important component to study. In that note, it may be concluded that the reflective nature of the Heliostats is very important in terms of the specular nature of reflection and the slope aspect of the receiver surface. Surface errors may be categorized as

a. Specular Errors: Specularity literally means mirror-like perfect reflection and it characterizes the angular dispersion of the irradiation. It works at microscopic level and causes shift of surfer normal from the desired direction as in fig. The chief cause of this errors may be categorized as absorption, scattering, Surface imperfection. Specularity errors may be mathematically written as

$$\Omega_{spec}^2 = k\Omega_{spec1}^2 + (1 - k)\Omega_{spec2}^2$$

where Ω_{spec1} is highly intense radiation with low specularity effect and Ω_{spec2} is low intense radiation with high specularity effect [78]

Reflective surfaces which are usually used for manufacture of heliostats are typically made of solar weighted specular reflectance of 90% to 95% [133].

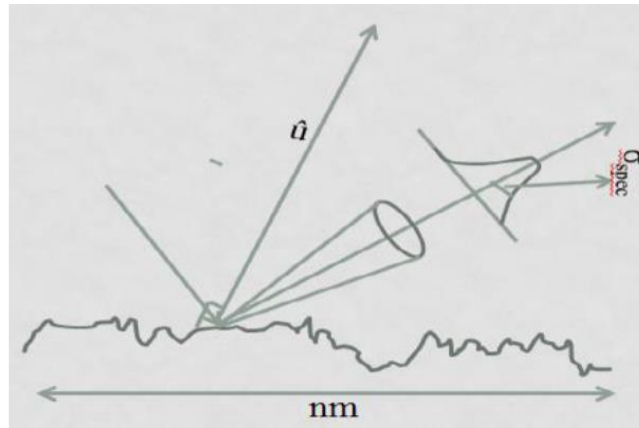


Fig 3.28 : Specularity error of surface

b. Slope Errors: Slope errors work at a macroscopic level as shown in fig and just like Specular errors, causes shift of the normal vector from the desired direction. The chief reason for this error may be categorized as deformation caused by gravitational effect wind effects, thermal loading and manufacturing imperfection [132]. Slope errors may be mathematically written in a two dimensional manner [131] as

$$\Omega_{sse} = \sqrt{\Omega_{sse,x}^2 + \Omega_{sse,y}^2}$$

Generally, Ω_{sse} is of the order of 1.5 mrad.[133]

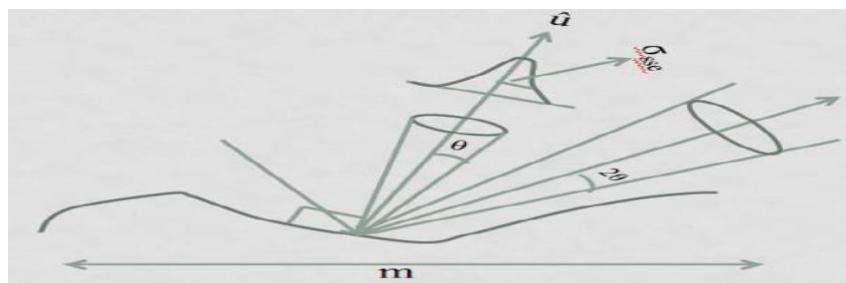


Fig 3.29 Slope error of surface

Usually the reflective errors are considered bivariate i.e they involve Specularity and Slope errors and they are dealt with radial standard deviation Ω_{bq} as below[134]

$$\Omega_{bq}^2 = \Omega_{spec}^2 + 4\Omega_{sse}^2$$

Losses, in this aspect of work do not happen individually but in an integrated fashion. It generates bad data and makes the system deviate from ideality.

3.9 Mathematics involved for generation of field layout

In Optics, ray is an idealized line of propagation of light which is perpendicular to the direction of wave front. In this theory, the entire light field of propagation is divided into countless number of rays. This makes the analysis and application of radiation logical. In homogeneous medium the ray direction are always straight. According to Fermat's principle, in a homogeneous medium, ray takes the minimum time to move from one point to other.

Geometrical optics guides the propagation of rays in a medium. Fig. (a) shows the principle of reflection on a reflective surface

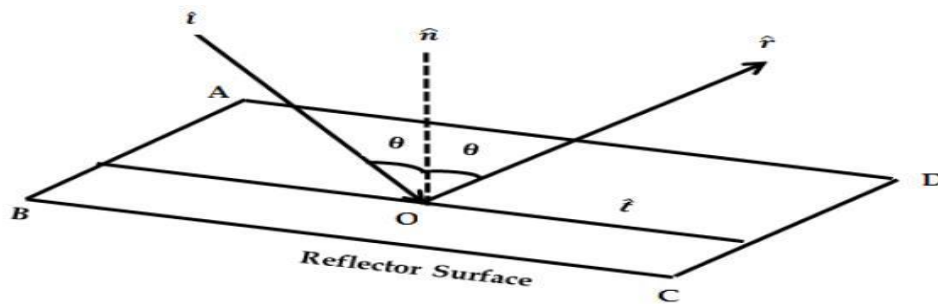


Fig 3.30 : Vector representation of laws of reflection

In fig 3.30, \hat{i} is the incident ray unit vector which hits a plane ABCD at O and gets reflected through the reflected ray unit vector \hat{r} . \hat{n} is the unit vector of the normal of plane ABCD at O and \hat{t} is a dummy vectors for calculation purpose.

The above diagram may be simplified as follows in figure

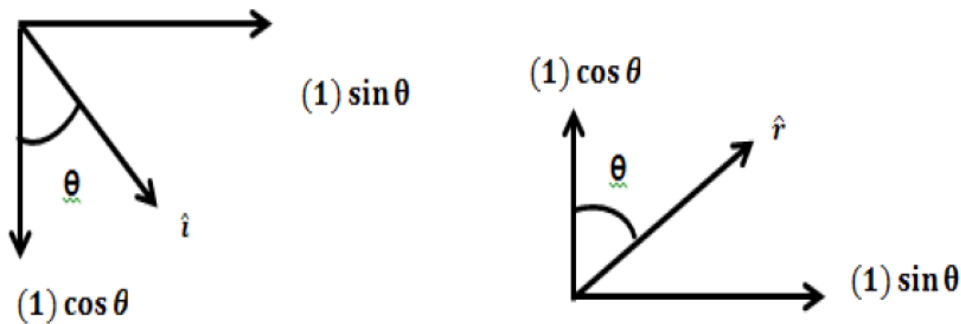


Fig 3.31 The incident ray (left) and the reflected ray (right) separately

The incident and reflected, vectorially, in collaboration with inputs from Fig 1 may be written as

$$\hat{i} = \sin \theta \hat{t} - \cos \theta \hat{n}$$

$$\hat{r} = \sin \theta \hat{t} + \cos \theta \hat{n}$$

Assembling the above two equations in the last page, the ray equation stand as

$$\hat{r} = \hat{i} - 2(\hat{i} \cdot \hat{n}) - \hat{n} \quad (3.17)$$

As laws of reflection are followed, Box product of irn must be zero, as they lie on the same plane

$$[\text{irn}] = \mathbf{i} \cdot (\mathbf{r} \times \mathbf{n}) = 0$$

3.9.1 Solar spatial coordinates

a) The polar coordinates were considered for the work in the following manner

A certain height of the receiver was considered for beam up work (For beam down work, the position of aim point is identical position). The \mathbf{r} coordinates for the set up was considered to be that position. Zenith and Azimuth angle of the Solar position were considered for the θ and φ for the polar coordinate system (r, θ, φ) .

b) To provide the (x, y, z) coordinate values to the software of work, the following conversion were done

$$\begin{aligned} x &= r \sin \theta \sin \varphi \\ y &= r \sin \theta \cos \varphi \\ z &= r \cos \theta \end{aligned}$$

As Cartesian coordinates are obtained, the solar point, in a plane manner, is expanded two dimensionally (x and y wise) to illuminate the entire field.

3.9.2 Solar angular coordinates

The heliostat field was considered to be in x-y plane with the receiver being vertically up along z axis. The following steps were followed to achieve the solar angular coordinates.

The distance unit vector between the solar point and heliostat point was calculated axis wise in the form of $\Delta x, \Delta y, \Delta z$.

The y axis angle of the solar point is calculated as

$$\tan \alpha = -90 - \frac{\sqrt{\Delta x^2 + \Delta y^2}}{\Delta z} \quad (3.18)$$

$$\tan \alpha = \frac{\Delta y}{\Delta x}$$

3.9.3 Heliostat spatial coordinates

As mentioned in section 3.5 and later in chapter 4 later, three manners of beam up and two manner of beam down were considered and performed. The coordinated of the central position of heliostats were considered in the following manner.

3.9.3.1 Radial Staggered

After calculation of the radial distance (ΔR) and (ΔA) as in equation, the following steps were taken to generate the solar field

a) The first row of heliostats i.e the first essential ring was to be placed at the same distance as that of the tower height

b) (ΔR) and (ΔA) in the subsequently ring and either side spread were done as $\frac{\Delta R}{2}$ and $\frac{\Delta Z}{2}$.

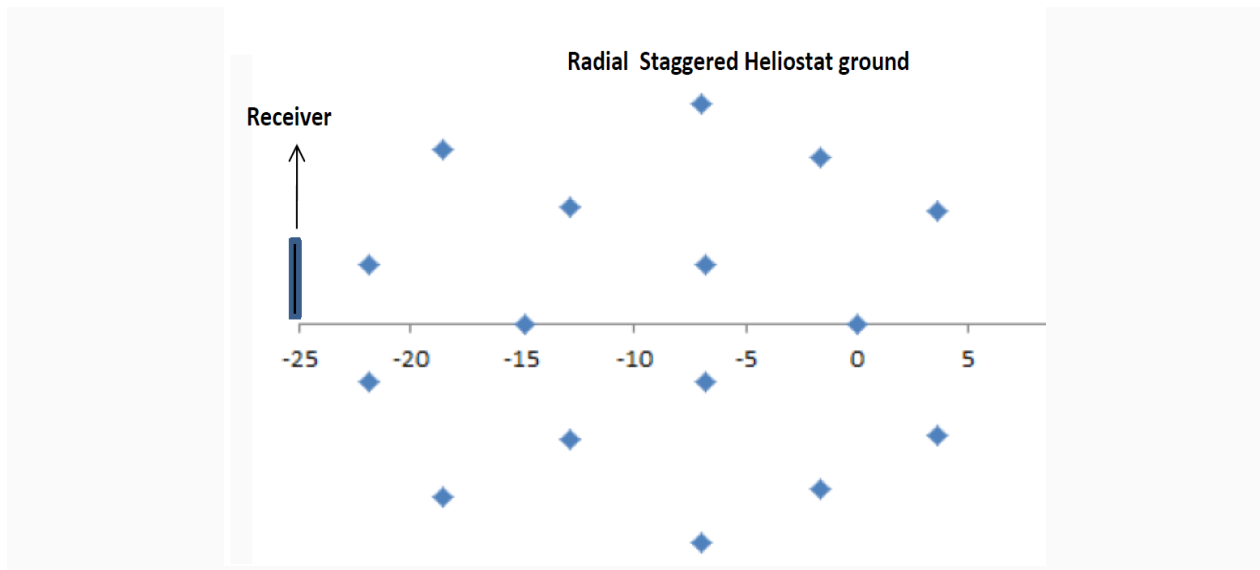


Fig 3.32 : Radial Staggered (RS) field set up

The first Heliostat on the above field under calculation is positioned at (0,0) and the rest as per Radial Staggered way as mentioned.

3.9.3.2 Cornfield

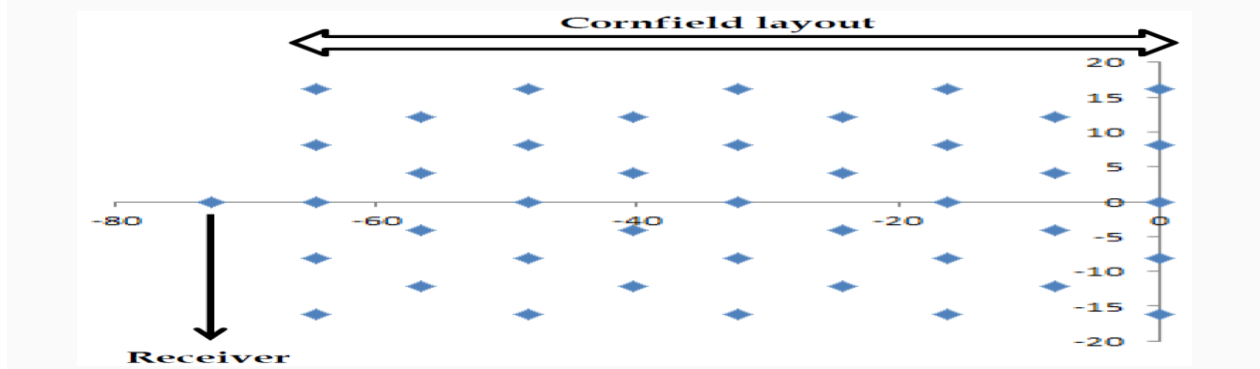


Fig 3.33 : Cornfield field set up

This field pattern, in a biometric pattern, is spread on ground in a identical manner in which the corns are spread for cultivation. To increase the field efficiency and reduce the established loses, two factors are considered as below

- a. The separation between the Heliostats.
- b. Dimension of Heliostats, in terms of metric values.

As done in RS pattern the distance between the first row of Heliostat and the foot of tower was kept same as the height of the tower.

Considering rectangular shaped Heliostat, DM is mathematically defined as [45]

$$DM = \sqrt{(m^2 + n^2)} + d \text{ where}$$

m is the length of Heliostat, n is the breadth of the Heliostat and d is the separation distance between the Heliostat.

Depending on the values of the factors as mentioned, the size of the field and power that generated is determined.

3.9.3.3 Sunflower

Sunflower or Fermat's spiral manner of field distribution is a biometric design where the heliostats are spread on the field in a Fermat's spiral pattern as shown below

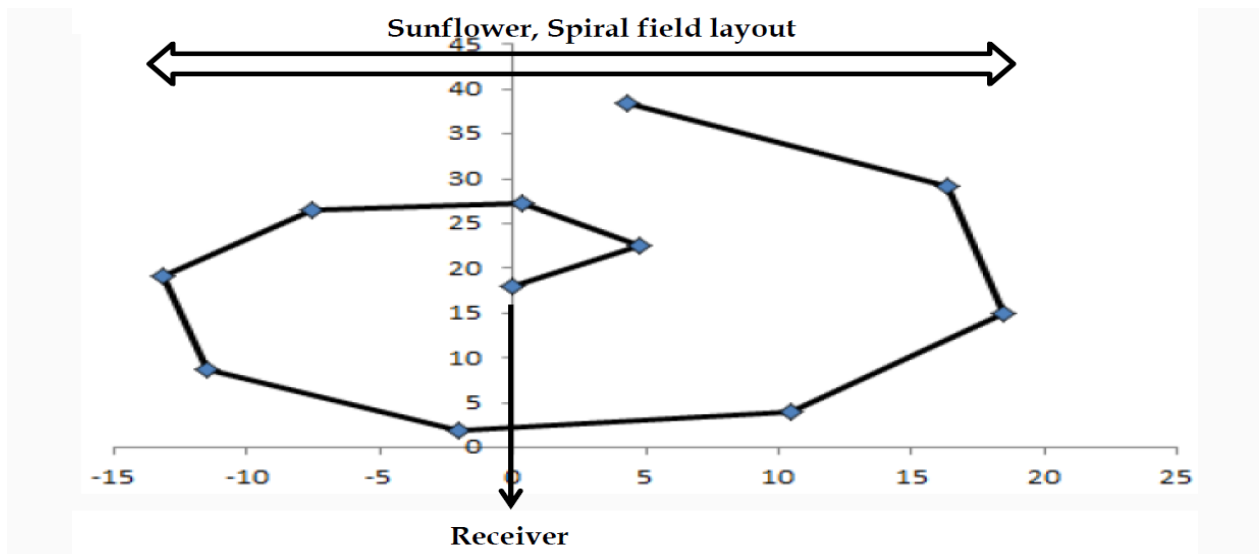


Fig.3.34 Sunflower design on ground, every dot represents a heliostat on ground.

The central heliostat is placed at (0,18),(18 being the height of the tower) and the rest of the heliostats are spread on the ground along xy direction.

The Fermat's Spiral algorithm as it was presented in^[8] generates heliostat fields based on spirals, based on continuous density function. Fermat spiral function represents the spirals as shown in sunflowers and thus the name. The position of a heliostat is defined as

$$\theta_k = 2\pi\phi^{-2}k$$

for the angular position and

$$r_k = ak^b$$

for the radial position. Therefore, this algorithm requires the following

- a. A linear Fermat's spiral parameter (a),
- b. A power Fermat's spiral parameter (b),

The heliostat dimensions, a formidable distance between heliostats, the heliostat minimum radial distance to the tower and the total number of heliostats are the required as input parameters.

3.9.4 Heliostat angles

Although in many a cases, the Heliostat are not tilted anywhere, it was found that tilting, preferably in a 2d manner, increase the efficiency of individual Heliostats. The solar radiation is captured in denser manner with Heliostat being aligned toward the receiver.

The tilting or rotation of the Heliostat plane are necessary to change the referral frame from that of Heliostat (x_1, y_1, z_1) to the receiver (x_2, y_2, z_2). For that purpose two methods as mentioned in the next two sub-sections are relevant.

3.9.4.1 Relationship between rotation angles and unit normal vector of the heliostat position

In this section, we elaborate how the rotational matrices help to propagate the reflected from the heliostat to the receiver position using ray tracing software Tracepro®. The normal vectors are the bisecting vectors between the incident ray and the reflected ray. In order to position the normal vector of the heliostat, it is necessary to identify the rotation matrix involved in the used software (Tracepro®) as used in this work. Among the possible fourteen (14) Euler rotation matrix [135], about x, y, z axis with α, β and γ are the respective angle of rotation about an axis. It was noted that the ray tracing software used in this work, uses the rotation matrix was of the form $R_{Total} = R_z R_y R_x$. The individual rotation matrices about each axis is defined as follows:

$$R_x(\alpha) = \begin{pmatrix} 1 & 0 & 0 \\ 0 & \cos \alpha & -\sin \alpha \\ 0 & \sin \alpha & \cos \alpha \end{pmatrix}$$

$$R_y(\beta) = \begin{pmatrix} \cos \beta & 0 & \sin \beta \\ 0 & 1 & 0 \\ -\sin \beta & 0 & \cos \beta \end{pmatrix}$$

$$R_z(\gamma) = \begin{pmatrix} \cos \gamma & -\sin \gamma & 0 \\ \sin \gamma & \cos \gamma & 0 \\ 0 & 0 & 1 \end{pmatrix}$$

The combination of the three axes of rotation will be as mentioned

$$R_{Total} = \begin{pmatrix} \cos \gamma \cos \beta & \sin \alpha \sin \beta \cos \gamma - \sin \gamma \cos \alpha & \sin \alpha \sin \gamma + \cos \alpha \cos \gamma \sin \beta \\ \sin \gamma \cos \beta & \sin \alpha \sin \beta \sin \gamma + \cos \gamma \cos \alpha & \sin \gamma \sin \beta \cos \alpha - \sin \alpha \cos \gamma \\ -\sin \beta & \sin \alpha \cos \beta & \cos \beta \cos \alpha \end{pmatrix}$$

The corresponding quaternions [136] may be written as

$$\begin{aligned} q_0 &= \sin \frac{\alpha}{2} \sin \frac{\beta}{2} \sin \frac{\gamma}{2} + \cos \frac{\alpha}{2} \cos \frac{\beta}{2} \cos \frac{\gamma}{2} \\ q_1 &= -\cos \frac{\alpha}{2} \sin \frac{\beta}{2} \sin \frac{\gamma}{2} + \sin \frac{\alpha}{2} \cos \frac{\beta}{2} \cos \frac{\gamma}{2} \\ q_2 &= \sin \frac{\alpha}{2} \cos \frac{\beta}{2} \sin \frac{\gamma}{2} + \cos \frac{\alpha}{2} \sin \frac{\beta}{2} \cos \frac{\gamma}{2} \\ q_3 &= -\sin \frac{\alpha}{2} \sin \frac{\beta}{2} \cos \frac{\gamma}{2} + \cos \frac{\alpha}{2} \cos \frac{\beta}{2} \sin \frac{\gamma}{2} \end{aligned}$$

The corresponding angles of (α, β, γ) may be obtained from R_{Total} and may be written as

$$\tan \alpha = \frac{R_{32}}{R_{33}}, \quad \tan \beta = \frac{-R_{31}}{\sqrt{1-R_{31}^2}}, \quad \tan \gamma = \frac{R_{21}}{R_{11}}$$

To consider i , r , n as the incident ray, reflected rays and normal to the surface of the heliostat concerned respectively. The incident ray vector i is defined by the solar position and the heliostat position (the solar position in this regard is taken that of Jodhpur, India (Lat :**26.24°** N ,Long : **73.02°E**)), the reflected ray vector r is defined by the heliostat position and the receiver position. Thus as the solar position change throughout the day as per Zenith and Azimuth, the unit normal vectors and hence them reflected ray vector were calculated in an hourly fashion for rays the to move from individual Heliostat to the receiver as per Eq 3.19.

The unit normal vector n , as mentioned is defined as the normal to the Heliostat surface. To achieve the reflected ray, the incident ray vector and the unit normal is mathematically satisfies the below relationship:

$$\hat{r} = \hat{i} - 2(\hat{i} \cdot \hat{n})\hat{n} \quad (3.19)$$

and the incident ray \hat{i} unit vector results are obtained mostly at an interval of one hour for 27th of every month in calendric year. The position of the heliostat according to field design is as described in section 3.5

Below is the matrix formulation to model the reflection from the heliostat. In ray tracing approach, each optical element may be represented by matrix [135]. In this formalism as the ray

propagates through system i.e it interacts with optical elements in the system, the output vector may be obtained as an outcome of matrix operations. Thus, using the matrix formalism, the output(O) i.e the final position vector for a given incident vector (I) may be obtained by the following relation

$$\hat{O} = M_{eff}\hat{I}$$

where M_{eff} is the effective matrix(s) corresponding of considered system of optical elements. The standard unit vector and its corresponding matrix may be represented as $\mathbf{n} = n_x\mathbf{i} + n_y\mathbf{j} + n_z\mathbf{k}$ and in matrix form it may be represented as

$$\mathbf{n} = \begin{bmatrix} n_x \\ n_y \\ n_z \end{bmatrix}$$

In an Heliostat field reflection happens as per laws of reflection and according to equation 3.19 and the unit normal vectors as mentioned. The matrix associated to each normal vector may be given as written as $\mathbf{M} = \mathbf{I} - 2\mathbf{nn}^T$ where n is mentioned above and \mathbf{n}^T is the transpose of it as in $[\mathbf{n}_x \ \mathbf{n}_y \ \mathbf{n}_z]$. This make the matrix M as below

$$\mathbf{M} = \begin{bmatrix} 1 & 0 & 0 \\ 0 & 1 & 0 \\ 0 & 0 & 1 \end{bmatrix} - 2[\mathbf{n}_x \ \mathbf{n}_y \ \mathbf{n}_z] \begin{bmatrix} \mathbf{n}_x \\ \mathbf{n}_y \\ \mathbf{n}_z \end{bmatrix}$$

$$\mathbf{M} = \begin{bmatrix} 1 - 2n_x^2 & -2n_xn_y & -2n_xn_z \\ -2n_xn_y & 1 - 2n_y^2 & -2n_yn_z \\ -2n_xn_z & -2n_yn_z & 1 - 2n_z^2 \end{bmatrix}$$

which satisfies equation 3.19. In the ray tracing software used in this work, the initial unit vector for the heliostat is in the z direction and the corresponding $\mathbf{n} = \begin{bmatrix} 0 \\ 0 \\ 1 \end{bmatrix}$ for any concerned heliostat with dimension of length a and breadth b. To suitably reflect the incident ray to the receiver, the heliostat is to be oriented and appropriate angle to be used as input. The angles which are to be given to any specified Heliostat were calculated as per Eq. with the unit normal vector given

$$\text{as } \mathbf{n} = \begin{bmatrix} n_x \\ n_y \\ n_z \end{bmatrix}$$

The corresponding y and z rotations were estimated using

$$\beta = \tan^{-1} \frac{\sqrt{n_x^2 + n_y^2}}{n_z} \text{ and } \gamma = \tan^{-1} \frac{n_y}{n_x}$$

and these values were used for precise positioning of Heliostats using the considered software.

A unit vector \mathbf{n} , where $\hat{\mathbf{n}} = n_x \hat{\mathbf{x}} + n_y \hat{\mathbf{y}} + n_z \hat{\mathbf{z}}$, if rotated about an axis with arbitrary angle θ then the rotation matrix $R(\mathbf{n}, \theta)$ may be written as

$$R(\mathbf{n}, \theta) = \begin{bmatrix} n_x^2(1 - \cos \theta) + (\cos \theta) & n_x n_y(1 - \cos \theta) - n_z \sin \theta & n_x n_z(1 - \cos \theta) + n_y \sin \theta \\ n_x n_y(1 - \cos \theta) + n_z \sin \theta & n_y^2(1 - \cos \theta) + (\cos \theta) & n_y n_z(1 - \cos \theta) - n_x \sin \theta \\ n_x n_z(1 - \cos \theta) - n_y \sin \theta & n_y n_z(1 - \cos \theta) + n_x \sin \theta & n_z^2(1 - \cos \theta) + (\cos \theta) \end{bmatrix}$$

The above equation is Rodrigue formula for 3x3 rotation $R(\mathbf{n}, \theta)$. Thus the rotation matrix associated for a given heliostat can be obtained either as R_{Total} or as $R(\mathbf{n}, \theta)$ depending upon the available information. In this investigation, the alignment of heliostats to the receiver were carried out using the methods discussed above.

3.9.5 Heliostat curvature

For curvatures on the Heliostat surface, in an individual manner, distance between individual Heliostat and the receiver is to be calculated. Considering that distance to be equal to focal length of Heliostat, curvature is to be introduced following the formula

$$Radius\ of\ Curvature(ROC) = 2 * Focal\ Lenth\ (FL) \quad 3.20$$

As the FL of the Heliostat changes from one to the other, so does the ROC

3.9.6 Conic

A conic may be considered of revolution formed by spinning a conic section, of a particular conic constant, around the axis. The details of this section was presented in sub section 3.3.2.

3.9.6.1 Hyperboloid equation used for Beam Down geometry

A hyperboloid is a section of a conic that may take the form of hyperbolas, ellipses, or circles. It is a quadric geometrical structure of two/three variables. It may consist of two sheets (three variable) called elliptical hyperboloid) or one sheet (two variables) called hyperbolic hyperboloid [137]. The eccentricity of a Hyperboloid is > 1 which makes the conic constant as -1 .

The general equation of a one sheet hyperboloid is written as below

$$\text{Equation: } \frac{x^2}{a^2} + \frac{y^2}{b^2} - \frac{z^2}{c^2} = 13.21$$

In case of axial length $2a$ and the coaxial length $2b$ at a distance l from the vertex, a and b being parametric constants, factor c may be defined as

$$c^2 = a^2 + b^2$$

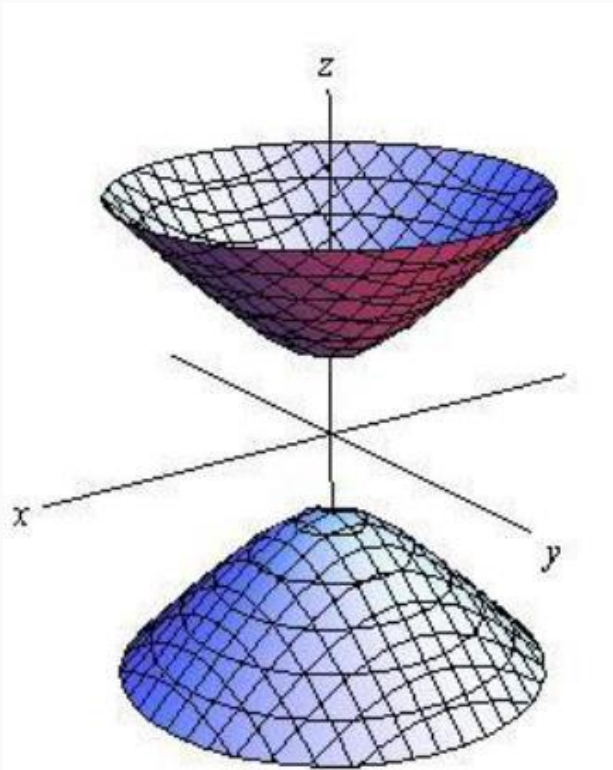


Fig.3.35 Hyperboloid model for Beam Down model [138]

The length of the hyperboloid is calculated from the vertex to the center of opening circle. The diameter/radius of the circle is variant and proportional to all the mentioned factor in the following equation

$$r^2 = b^2 \left[\frac{(l+z)^2}{a^2} - 1 \right] \quad (12.5)$$

3.9.6.2 Ellipsoid equation used for Beam Down geometry

Another conic section used for the beam down model is that of two sheet ellipsoid, although as shown in Fig 3.12 only one sheet is operated for this work as in Fig 4.17. Its geometric structure has two foci which is used for the beam down modelling. The Heliostats on the ground are targeted to one of the foci and the ellipsoid interior surface, based on geometry, forces the rays to approach the second foci. The first focal point is the aim point and the second is the receiver position. The eccentricity of a Ellipsoid is between 0 and 1 which makes the conic constant as between -1 and 0.

3.10 NON-IMAGING OPTICS (NIO)

Imaging Optics is, broadly speaking, based on image-formation using lens and mirrors together with filters and other optical components. It works on the principle of point-to-point correspond between source and image for imaging which is a constraint of work otherwise.

NIO is an approach of using optical devices for collection, concentration, and transport of light from the source to receiver [138-141]. This approach permits the design of optical systems to obtain the maximum geometric concentration permitted theoretically and thermodynamically. Collection of as much as light as possible using physical conservation laws for a given angular field of view was the object of work. A hybrid structure as has been shown in Beam Down work increasing the efficiency.

Prior to the development of NIO it was considered that no useful concentration could be achieved without tracking the solar radiation i.e without following the moving Sun[139]. Tracking may be necessary/used as a hybrid way of work if high concentration is necessary, which otherwise, for moderate concentration, allows great relaxation in optical tolerances and/or the achievement of higher concentrations within the same tolerances limit.

The Compound Parabolic Concentrator (CPC) invented by Roland Winston in 1974 is considered the '**Ideal**' non-imaging optical light collector and is considered a generic term for the whole family of similar devices [139] and often called Winston Cone.

There are relevant differences between non-imaging optics and conventional imaging/focusing optics. The underlying formalism of NIO is based on analysis of light propagation in terms of phase space quantities and/or energy flow patterns. In NIO, the optical elements (mirrors/lenses) are designed in such a manner that the extreme angular rays rather than for axial rays of the desired field of view are collected. Rays that are closer to the axis are not brought to a focal point, but all are nevertheless collected. Such non-imaging properties of these systems may approach and, in some cases, attain the thermodynamic limit for concentration as mentioned in eq. which otherwise imaging i.e focusing system for short of by a factor of 3-10

3.10.1 Advantages of NIO for solar energy concentration

a.NIO have an advantage of achieving a wide angular field of view for a given geometric concentration. This permits useful concentration without even tracking.

b.Low to moderate concentrations (with a factor 1.1 to 2 and in some cases even 4) can be achieved with a totally stationary (i.e fixed year-round) collector. Higher levels (3 to 10 and above) usually require occasional (preferably seasonal) adjustment.

c.High concentration i.e a factor above 10will require addition tracking together with NIO. However, as an advantage with NIO techniques, these factors of concentration may be obtained with relaxed optics and tracking requirements.

d. Generally NIO offer simpler, economic, and more easily maintained concentrator systems.

3.10.3 Edge-Ray algorithm to generate a CPC

The edge ray principle states that when the light rays coming from the edges of the source are redirected towards the edges of the receiver, this will ensure that all light rays coming from the inner points in the source will end up on the receiver. There is no condition on image formation, the only goal is to transfer the light from the source to receiver. As this optical principle is not targeted to form a proper image (one - to - one correspondence), scrambling of rays is not supposed to disturb the process, as long as the energy content of the source (i.e the collector/ Heliostat in this case) is transferred to the receiver. The figure 3.36 in the next page illustrates CPC as non-imaging optics.

According to Fermat's principle, the optical path length between object and image points are the same for all rays irrespective of imaging and non-imaging properties of the device concerned. As shown in Fig 3.36 this principle is applied to the rays to attain the edge-ray algorithm of non-imaging optical design as shown in mentioned Figure. One end of a ray hitting the point A may be considered tilted at angle θ to the entrance aperture AB and tied to the other end to the edge of the exit aperture CD.

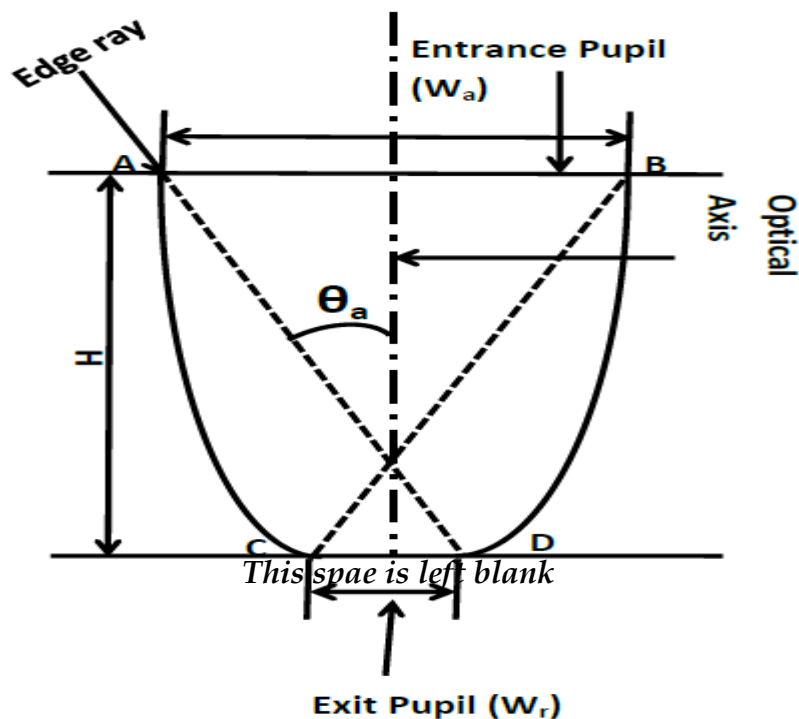


Fig 3.36 : Compound Parabolic Concentrator (2d) [139,140]

From figure 3.36

$$CD = AB \sin \theta_a$$

This construction would give a 2D compound parabolic concentrator (CPC). Rotating the profile about the axis of symmetry would generate the 3D CPC with radius (a) at the entrance and (b) at the exit. The 2D CPC is an ideal concentrator – that is, it works perfectly for all rays within the acceptance angle θ (in 2D geometry). The optical length of the string was kept fixed in the above design.

Focal length of this structure was calculated as

$$f = \frac{DC}{2}(1 + \sin \theta_a)$$

The overall height of the structure may be written as

$$H = \frac{f \cos \theta_a}{\sin^2 \theta_a}$$

3.10.4 Invariance, Etendue and Solar Concentration

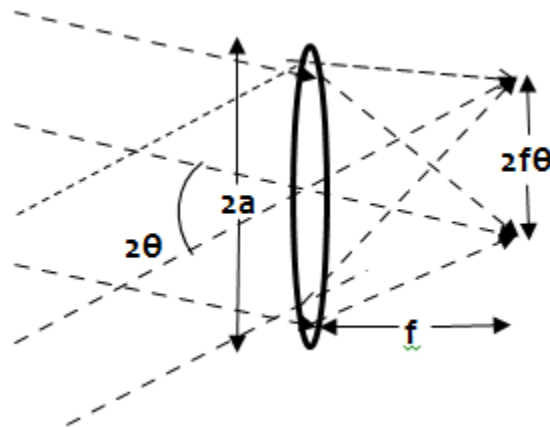


Fig 3.37: Imaging Optics to form an image at the back focal plane i.e Lens of focal length f generating image of size $2f\theta$

Rays in the above figure are considered to traverse from left to right with source being of finite size at a great distance. Every point on the source diverges at an angle i.e the angular extent is 2θ , passes through the imaging element, convex lens in the above case, and converge to form an image of size $2f\theta$. The diameter of the lens is taken to be $2a$. The rays are considered to be axial they pass through the lens without much deviation.

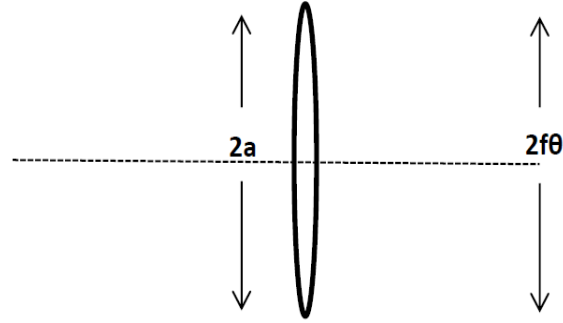


Fig 3.38: Imaging Optics

The above two figure shows one of the most fundamental concepts that is used in concentrator theory i.e., the concept of a beam of light of a certain diameter ($2a$ in this case) and angular extent (2θ in this case). Considering a flux of radiation on the back focal plane with radiation being off-axis, the size of the image is θa (ignoring the factor 4). This quantity i.e θa is known in various names like extent, etendue, acceptance, and Lagrange invariant [39]. It is an invariant through the optical system with no obstructions in the light beam passage and when certain losses due to properties of the materials, such as absorption and scattering are ignored.

It is the square of this quantity i.e $\theta^2 a^2$, also called etendue, which is the invariant of optical passage signature.

Considering an aperture of diameter $2f\theta$ at the focal plane of the lens, as in fig.3.37, the system would accept only rays within the angular range of $\pm\theta$ and inside the diameter $2a$. Considering flux of radiation B being incident on the lens from the left, the system will accept a total flux $B\pi^2\theta^2 a^2$. In this connection, the étendue or acceptance $\theta^2 a^2$ is considered as a measure of the power flow that passes through the system. Using these two figures above, the entire power $B\pi^2\theta^2 a^2$ may be considered to flow to the right of the setup considering the input aperture to be $2f\theta$ diameter.

So, the concentration ratio may be written as

$$C = \left\{ \frac{2a}{2f\theta} \right\}^2 = \left\{ \frac{a}{f\theta} \right\}^2$$

When the radiation is considered to be in a medium of index n , the invariant takes the form of $n^2\theta^2 a^2$, the reason being in that Snell's law is to be considered.

The half angle spread of solar radiation, as mentioned, is 4.67 mrad. For 3-dimensional (3D) concentrators

$$C = \left\{ \frac{n}{\sin\theta} \right\}^2$$

Considering $n = 1$ and θ as mentioned, C turns out as ≈ 44000 and is the maximum concentration possible

In this manner, the theoretical sine law limit of concentration is approached with high throughput.

3.10.5 Geometrical Concentration Factor (GCF)

A solar concentrator is an optical device that accepts direct solar radiation on an aperture with certain area A_C , called Collector and reflects that to another aperture A_R , called Fig receiver.

$$\text{GCF} = \frac{A_C}{A_R}$$

As evident in eq ,to increase the GCF, the size of the receiver is kept small.

Optical Concentration is the average irradiance integrated over the entire receiver surface area divided by the irradiance incident on the collector aperture.

Thermal Concentration is the concentration of solar irradiation on an absorber surface in terms of a reflective surface which receives direct solar radiation. The object of concentration is to produce high temperature on the absorber surface

This space is left blank